

AD A 039176

2

FG



AD

AMMRC CTR 77-14

3-D STRESS ANALYSIS OF A TURBINE BLADE

March 1977

C. M. LEWIS, R. A. SAMUEL, and F. YEN
Boeing Aircraft Company
P. O. Box 3707, Seattle, Washington 98124

Final Report Contract Number DAAG46-75-C-0072

Approved for public release; distribution unlimited.

Prepared for
U.S. ARMY AVIATION SYSTEMS COMMAND
St. Louis, Missouri 63166

ARMY MATERIALS AND MECHANICS RESEARCH CENTER
Watertown, Massachusetts 02172



AD NO. _____
DDC FILE COPY

The findings in this report are not to be construed as an official Department of the Army position, unless so designated by other authorized documents.

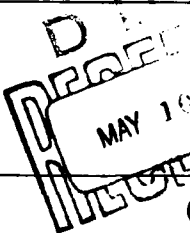
Mention of any trade names or manufacturers in this report shall not be construed as advertising nor as an official indorsement or approval of such products or companies by the United States Government.

DISPOSITION INSTRUCTIONS

Destroy this report when it is no longer needed.
Do not return it to the originator.

UNCLASSIFIED

SECURITY CLASSIFICATION OF THIS PAGE (When Data Entered)

REPORT DOCUMENTATION PAGE		READ INSTRUCTIONS BEFORE COMPLETING FORM
1. REPORT NUMBER 13 AMMRC CTR-77-14 ✓	2. GOVT ACCESSION NO.	3. RECIPIENT'S CATALOG NUMBER
4. TITLE (and Subtitle) 3-D STRESS ANALYSIS OF A TURBINE BLADE ✓	5. TYPE OF REPORT & PERIOD COVERED 9 Final Report ✓	
7. AUTHOR(s) C. M. Lewis, R. A. Samuel, F. Yen	6. PERFORMING ORG. REPORT NUMBER 14 D6-42735 ✓	
9. PERFORMING ORGANIZATION NAME AND ADDRESS Boeing Commercial Airplane Co. ✓ Propulsion Technology Unit Seattle, Washington 98124	8. CONTRACT OR GRANT NUMBER(s) 15 DAAG46-75-C-0072 NEW	
11. CONTROLLING OFFICE NAME AND ADDRESS U.S. Army Air Mobility Research & Development Lab. ATTN: SAVDL-LE-T, Lewis Directorate, NASA-Lewis Research Center, Cleveland, Ohio 44135	10. PROGRAM ELEMENT, PROJECT, TASK AREA & WORK UNIT NUMBERS AMCMS Code: 798017.A50Q3019-MS-3MS	
14. MONITORING AGENCY NAME & ADDRESS (if different from Controlling Office) Army Materials and Mechanics Research Center Watertown, Massachusetts 02172	12. REPORT DATE 11 Mar 5 1977	
16. DISTRIBUTION STATEMENT (of this Report) Approved for public release; distribution unlimited.	13. NUMBER OF PAGES 77 12801	
17. DISTRIBUTION STATEMENT (of the abstract entered in Block 20, if different from Report)	15. SECURITY CLASS. (of this report) Unclassified	
18. SUPPLEMENTARY NOTES	15a. DECLASSIFICATION/DOWNGRADING SCHEDULE	
19. KEY WORDS (Continue on reverse side if necessary and identify by block number) Stress analysis Finite element method Gas turbine blades	<div style="text-align: right;">  <p>DRAFT MAY 10 1977 MILITARY C</p> </div>	
20. ABSTRACT (Continue on reverse side if necessary and identify by block number) (SEE REVERSE SIDE)		

DD FORM 1 JAN 73 1473

EDITION OF 1 NOV 65 IS OBSOLETE

UNCLASSIFIED

SECURITY CLASSIFICATION OF THIS PAGE (When Data Entered)

3902

UNCLASSIFIED

SECURITY CLASSIFICATION OF THIS PAGE(When Data Entered)

Block No. 20

ABSTRACT

This report presents a demonstration of the usefulness of the ATLAS system in performing three-dimensional elastic stress analysis of a turbine blade.

Modeling details for a shrouded uncooled turbine blade are outlined and program execution and data management techniques are discussed.

It was concluded that three-dimensional elastic stress analysis provides an accurate means of predicting stresses in a complex structure. However, high computer costs require that this method of stress analysis be used with discretion. Areas for further study are suggested.

UNCLASSIFIED

SECURITY CLASSIFICATION OF THIS PAGE(When Data Entered)

FOREWORD

This work was carried out as an aid to performance studies of the T55-L-M engine for the CH-47 helicopter. The work was performed by the Propulsion Technology Unit of Boeing Commercial Airplane Co., Seattle, Washington. Support for the effort was provided by the CH-47 Modernization Program Office of the U. S. Army Aviation Systems Command, St. Louis, Missouri, through the Lewis Directorate of the Air Mobility Research and Development Laboratory, NASA-Lewis Research Center, Cleveland, Ohio. Monitoring effort was provided by the Mechanics Research Laboratory of the Army Materials and Mechanics Research Center, Watertown, Massachusetts.

CLASSIFIED BY

NOIS

DATE

UNCLASSIFIED

JUSTIFICATION

BY

DISTRIBUTION AVAILABILITY CODES

CLASS.	AVAIL.	OR	SPECIAL
A			

White Section

Buff Section

3-D STRESS ANALYSIS OF A TURBINE BLADE

D6-42735

C. M. Lewis
R. A. Samuel
F. Yen

December 1975

Prepared under Contract DAAG46-75-C-0072

by

Boeing Commercial Airplane Company
P.O. Box 3707
Seattle, Washington 98124

for

ARMY MATERIALS AND MECHANICS RESEARCH CENTER
Watertown, Massachusetts 019040

J15-047

CONTENTS

	<u>Page</u>
LIST OF ILLUSTRATIONS	iii
LIST OF TABLES	vi
SYMBOLS AND ABBREVIATIONS	vii
SUMMARY	7
1.0 INTRODUCTION	2
2.0 THE ATLAS PROGRAM	3
3.0 THE BLADE MODEL	5
4.0 PROGRAM EXECUTION	17
5.0 STRESS CONTOUR PLOTS	19
6.0 TWO- AND THREE-DIMENSIONAL ANALYSIS COMPARISONS	32
7.0 CONCLUSIONS AND RECOMMENDATIONS	37
APPENDIX A ATLAS OUTPUT	39
APPENDIX B STRESS CONTOUR PLOTS	43

D1 4100 374C OR.G. 3/71



J18-CA7

LIST OF ILLUSTRATIONS

<u>Figure</u>		<u>Page</u>
3.1	Turbine Blade Geometric Model	6
3.2	Stiffness Data Set 1	8
3.3	Typical Fir Tree Section Map	9
3.4	Stiffness Data Set 5	10
3.5	Stiffness Data Set 6	11
3.6	Stiffness Data Set 3	12
3.7	Stiffness Data Set 4	13
3.8	Root Boundary Conditions and Coordinate Systems	14
3.9	Tip Shroud Boundary Condition	14
5.1	Radial Stress, CF Load, Pressure Side	20
5.2	Radial Stress, CF Load, Suction Side	21
5.3	Radial Stress, Aero Load, Pressure Side	22
5.4	Radial Stress, Aero Load, Suction Side	23
5.5	Radial Stress, Thermal Load, Pressure Side	24
5.6	Radial Stress, Thermal Load, Suction Side	25
5.7	Radial Stress, Tip Rub Load, Pressure Side	26
5.8	Radial Stress, Tip Rub Load, Suction Side	27
5.9	Radial Stress, CF + Aero + Thermal Loads, Pressure Side	28
5.10	Radial Stress, CF + Aero + Thermal Loads, Suction Side	29
5.11	Radial Stress, CF + Aero + Thermal + Rub Loads, Pressure Side	30
5.12	Radial Stress, CF + Aero + Thermal + Rub Loads, Suction Side	31

D1 4100 7740 ORIG 3/71



J 16-047

LIST OF ILLUSTRATIONS (cont'd)

<u>Figure</u>		<u>Page</u>
6.1	Boundary Conditions for NASTRAN 2-D Analysis	33
6.2	Boundary Conditions for ATLAS 3-D + NASTRAN 2-D Analysis	33
6.3(a)	Pressure Side Stress Comparison	34
6.3(b)	Suction Side Stress Comparison	34
6.4	Predicted Maximum Stress vs. Failure Point Comparison	36
B.1	Equivalent Stress, CF Load, Pressure Side, Set 6	44
B.2	Equivalent Stress, CF Load, Suction Side, Set 6	45
B.3	Equivalent Stress, Aero Load, Pressure Side, Set 6	46
B.4	Equivalent Stress, Aero Load, Suction Side, Set 6	47
B.5	Equivalent Stress, Thermal Load, Pressure Side, Set 6	48
B.6	Equivalent Stress, Thermal Load, Suction Side, Set 6	49
B.7	Equivalent Stress, Tip Rub Load, Pressure Side Set 6	50
B.8	Equivalent Stress, Tip Rub Load, Suction Side Set 6	51
B.9	Equivalent Stress, CF + Thermal + Aero Loads, Pressure Side, Set 6	52
B.10	Equivalent Stress, CF + Thermal + Aero Loads, Suction Side, Set 6	53
B.11	Equivalent Stress, CF + Aero + Thermal + Rub Loads, Pressure Side, Set 6	54

D1 4100 7740 ORIG. 2/71

J18-47

LIST OF ILLUSTRATIONS (cont'd)

<u>Figure</u>	<u>Page</u>
B.12 Equivalent Stress, CF + Aero + Thermal + Rub Loads, Suction Side, Set 6	55
B.13 Equivalent Stress, CF Load, Pressure Side, Set 3	56
B.14 Equivalent Stress, CF Load, Suction Side, Set 3	57
B.15 Equivalent Stress, Aero Load, Pressure Side, Set 3	58
B.16 Equivalent Stress, Aero Load, Suction Side, Set 3	59
B.17 Equivalent Stress, Thermal Load, Pressure Side, Set 3	60
B.18 Equivalent Stress, Thermal Load, Suction Side, Set 3	61
B.19 Equivalent Stress, Tip Rub Load, Pressure Side, Set 3	62
B.20 Equivalent Stress, Tip Rub Load, Suction Side, Set 3	63
B.21 Equivalent Stress, CF + Aero + Thermal Loads, Pressure Side, Set 3	64
B.22 Equivalent Stress, CF + Aero + Thermal Load, Suction Side, Set 3	65
B.23 Equivalent Stress, CF + Aero + Thermal + Rub Load, Pressure Side, Set 3	66
B.24 Equivalent Stress, CF & Aero + Thermal + Rub Load, Suction Side, Set 3	67

D1 4100 7740 ORIG. 3/71



J15-47

LIST OF TABLES

<u>Table</u>		<u>Page</u>
3.1	Substructure Description	7
3.2	Temperature vs. Z-Coordinate	15
3.3	Blade Pressures	16
A.1	Computation Time and Resources	40

D 1 4100 7740 ORIG. 3/71



21E-747

SYMBOLS AND ABBREVIATIONS

Symbol

CF	Centrifugal force	lb, (N)
R	Radius	inches, (m)
psi	Stress or pressure	lb/in. ² , (N/m ²)
ksi	Stress	1000 lb/in. ² , (N/m ²)
θ_z	Angle of rotation about Z-axis	radians

D1 4100 7740 ORIG. 3/71

115-47

SUMMARY

This report presents a demonstration of the usefulness of the ATLAS system in performing three-dimensional elastic stress analysis of a turbine blade.

Modeling details for a shrouded uncooled turbine blade are outlined and program execution and data management techniques are discussed.

It was concluded that three-dimensional elastic stress analysis provides an accurate means of predicting stresses in a complex structure. However, high computer costs require that this method of stress analysis be used with discretion. Areas for further study are suggested.

D1 4100 7740 ORIG. 3/71



JIR-C47

1.0 INTRODUCTION

Assessment of the state of stress in solid structures has long been the goal of stress analysts. However, three-dimensional stress methods have been limited, for the most part, to photoelastic methods which provide good results for a very limited number of loading types. For example, analysis of turbine blades has been limited to centrifugal loading because thermal and aerodynamic loadings have been difficult or impossible to simulate by photoelastic methods.

In recent years the stiffness method of finite element stress analysis has provided a solution for three-dimensional stress analysis through the isoparametric solid element (ref. 1). Since 1968 there has been a proliferation of finite element programs, both public and proprietary, which incorporate some form of the three-dimensional isoparametric solid element. The ATLAS System (ref. 2) is one such program, available to government agencies and certain of their contractors, which provides the user with a highly versatile isoparametric brick family.

However, users soon found that something more than an accurate finite element was necessary for a successful three-dimensional stress analysis. Even relatively simple three-dimensional models can produce very large and costly computational problems which may exceed the capacity of the largest computers. It became evident that an efficient data management system and substructuring capability were as important as the finite element itself for a successful three-dimensional stress analysis.

This study was undertaken to demonstrate the usefulness of the ATLAS system in executing an elastic stress analysis of a turbine blade. The problem selected required use of the system's isoparametric element family, various loading options, data management features, and automated substructuring capability, all of which are essential for successful execution of moderate to large three-dimensional stress analyses.

The authors gratefully acknowledge the support of the program manager, M. Aarnes and of the ATLAS Staff in accomplishing the goals of this document.

DI 4100 7740 ORIG. 3/71



2.0 THE ATLAS SYSTEM

ATLAS is an integrated structural analysis and design system operational on the Control Data Corporation (CDC) 6600/CMBER computers. It is a modular system of computer codes integrated within a common executive and data base framework. The system has a broad scope in that its analytical capabilities support many different but related aeroelastic technological disciplines. However, in this report, ATLAS will be discussed only in its role as a three-dimensional elastic stress analysis tool.

The element selected for this demonstration is the isoparameter brick element. The ATLAS brick element family is composed of four major elements with orthotropic material properties. They are the linear, quadratic, cubic and quartic bricks. That is geometry, displacement, thermal strains, and pressures are expressed as linear through quartic polynomials along the edges of the brick. Each element is defined by 3 corner nodes and 12 edges each of which may have up to 3 intermediate nodes. Nodes are allowed 3 translatory degrees of freedom.

Loadings provided by ATLAS include any or all of the following:

- a) Inertia loads
- b) Point loads
- c) Pressure loads
- d) Thermal loads
- e) Specified displacements

Centrifugal loading, which is a special case of the inertia loading option, is accomplished by defining a rotation vector which provides both direction and angular velocity of the rotation. The number of load cases in a given analysis is limited only by the capacity of the computer system used.

Three types of coordinate systems are available to the user. These are the rectangular, cylindrical and spherical systems. Any number of each may be used within a problem to define both input and analysis reference frames. Thus, complex geometries and supported and specified boundary conditions may be conveniently selected by the user in order to simulate nearly any real situation.

Element stresses in terms of 3 normal and 3 shear stresses are computed for the global coordinate system at the element centroid. The user may also request that stress at the nodes be printed instead of or in addition to the centroidal stresses.



Computational module control is maintained by the user via a concise technically oriented language which may include a FORTRAN program used for auxiliary processing.

The reader is referred to the ATLAS Users Manual (ref. 2) for a more detailed description of the system.

D1 8100 7740 ORIG. B/71



J15-247

3.0 THE BLADE MODEL

This section describes the geometric and loading models generated for a shrouded, uncooled power turbine blade. Blade geometry, metal temperature, and gas pressures were provided by Lycoming Division of the AVCO Corporation. The subject blade had previously undergone a partial three-dimensional analysis in which a portion of the blade was modeled three-dimensionally and the remainder modeled two-dimensionally. It was the goal of the current study to provide a more detailed, fully three-dimensional stress analysis of the blade and thereby demonstrate the usefulness of the ATLAS system in three-dimensional stress analysis.

The original three-dimensional model of the blade included that portion of the blade from .5 inch above the platform down through the first serration of the fir tree. Force boundary conditions from a two-dimensional model were applied to the top of the model and support boundary conditions were applied to the fir tree.

The current model was built from the original by adding the remainder of the fir tree, the airfoil, and the tip shroud. Element corner node numbers from the original three-dimensional model were retained in the updated model, but the element definition of the original section was upgraded from 20 or 24 node bricks to 32 node bricks. The purpose of the refinement was to more accurately determine the stresses in the area of the blade root fillet. The addition to the fir tree was modeled with 32 node bricks and the airfoil and tip shroud were modeled with 8 node bricks. The full blade model was then substructured as shown in figure 3.1.

The decision to use substructures was made at the outset in order to allow for subsequent modifications to boundary conditions and tip loads. However, it was found during execution of the problem that substructuring would have been necessary in any case to reduce the problem size to fit the production configuration of the Boeing Computer Services (BCS), CDC 6600 computer. That problem is discussed in more detail in section 4.0.

Each substructure was defined by a corresponding stiffness data set containing nodal point coordinates and element definitions. The substructure numbers and data set numbers together with other pertinent data are given in table 3.1.

D14100 7740 ORIG. 2/71



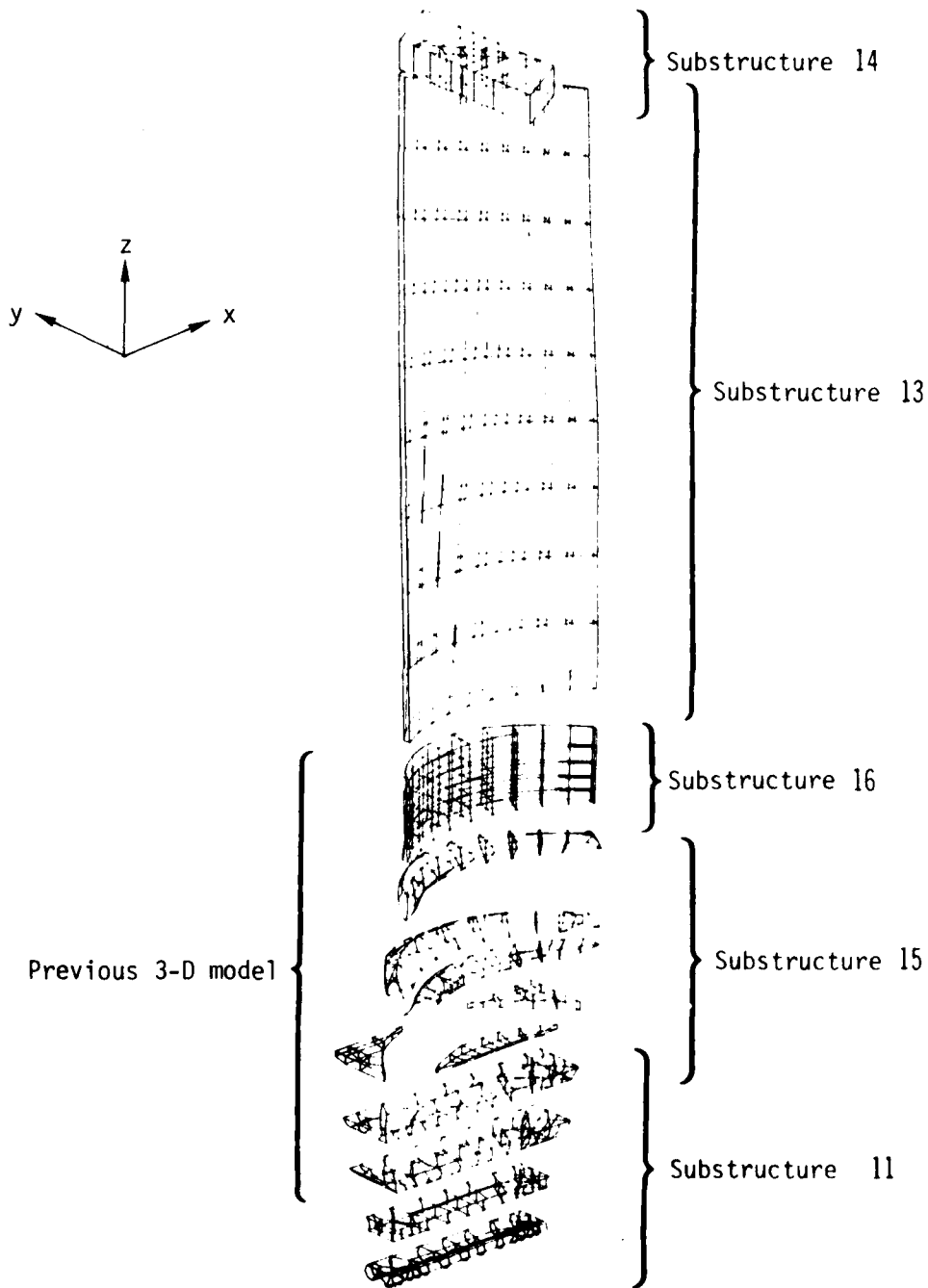


Figure 3.1 Turbine Blade Geometric Model

Table 3.1 Substructure Description

Substructure number	11	13	14	15	16	21
Stiffness data set	1	3	4	5	6	--
Number of nodes	1076	219	57	895	953	315
Number of elements	92	81	23	66	90	--
Nodes per element	32	8	8	32	32	--
Retained nodes	145	46	16	269	154	--
Free freedoms	2616	510	120	1869	2388	945
Retained freedoms	435	138	48	807	462	--
Supported freedoms	132	0	2	0	0	--
Average half bandwidth	848	86	76	1281	732	531

Maps of each substructure together with element corner node numbers are given in figures 3.2 and 3.4-3.6. Element numbers in data set 1 were generated by adding the two least significant digits from one of the node numbers on the element upper face to an integer equal to or greater than 4200. This method may be demonstrated by observing the fir tree section map shown in figure 3.3 in conjunction with figure 3.2. One may obtain any of the element numbers in data set 1 by using the prefixes given in figure 3.2 and adding the integers found encircled in figure 3.3. Element numbers for data sets 5 and 6 correspond to a node number usually found in the second quadrant of the element upper face.

The stiffness data set information was checked for accuracy via the plot postprocessors found in the ATLAS system. Additional checking for some of the more complex geometries was done on Vector General 3-D Vector scope driven by a PDP 11/45 computer.

The global coordinate system used for nodal point definition was a right-hand rectangular coordinate system with the x-axis as the center line of the engine (positive aft), the y-axis as the tangential direction, and the z-axis as the blade stacking axis. Two additional coordinate systems were used for purposes of boundary condition specifications. The x-axis of the systems lay parallel to the longitudinal axis of the fir tree (positive aft). The pressure side system was rotated 45° about its x-axis, while the suction side system was rotated -45° about its x-axis. These systems appear in the ATLAS coordinate system definitions as ROOTPS and ROOTSS respectively, and are shown in figure 3.8. Note that the fir tree lands were free to slide parallel to the contact surface. No shearing forces were allowed.

The tip shroud boundary condition allowed translations in all directions but no rotation about the global z-axis. This was accomplished by attaching 8 massless beams with stiffness properties defined in the x-y plane only from each of the corners of the tip shroud to 2 nodal points on the upper and lower surfaces of the tip shroud at the intersection with the z-axis as shown in figure 3.9. The 2 nodal points were constrained against rotation about the z-axis.

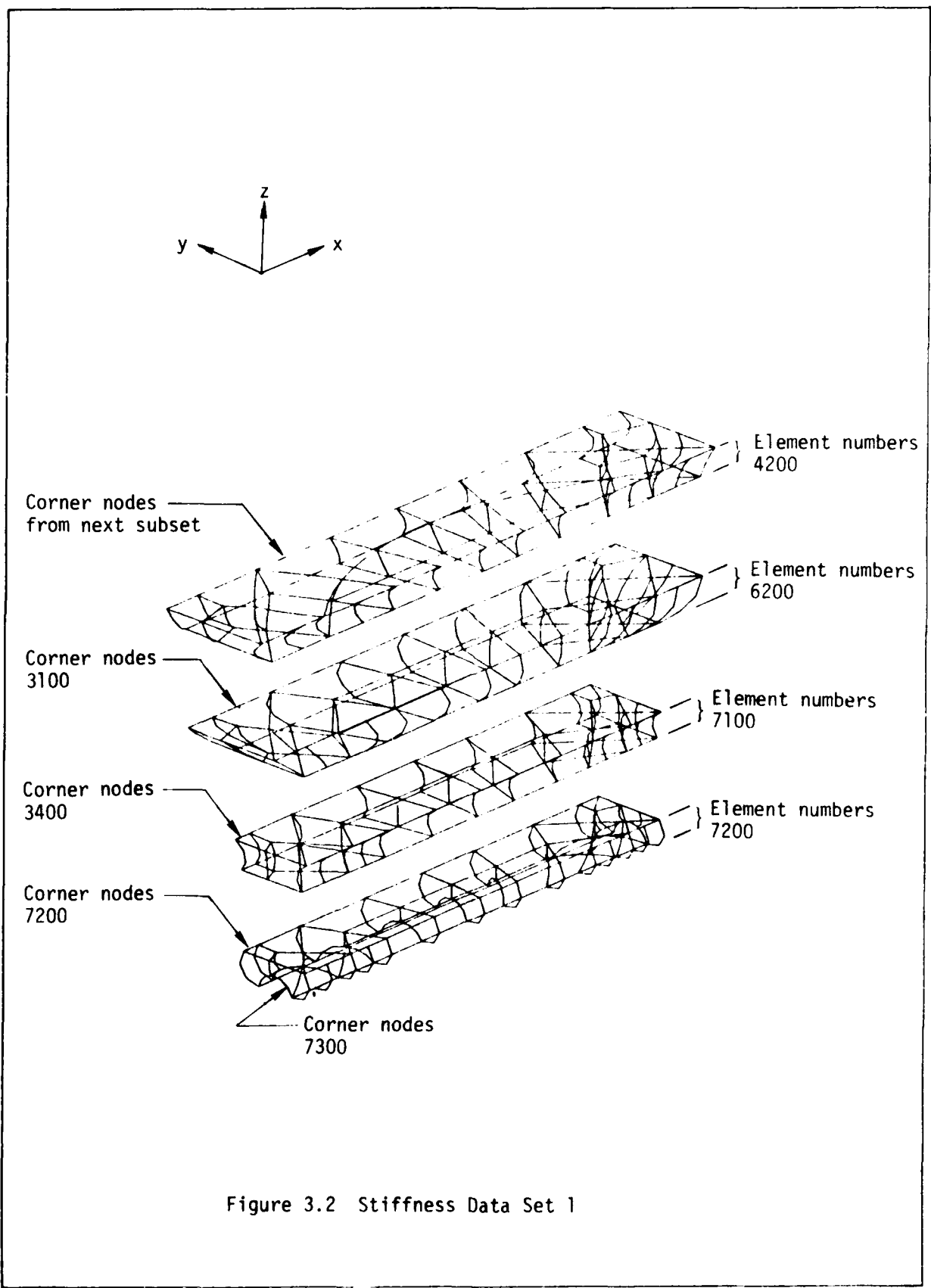


Figure 3.2 Stiffness Data Set 1

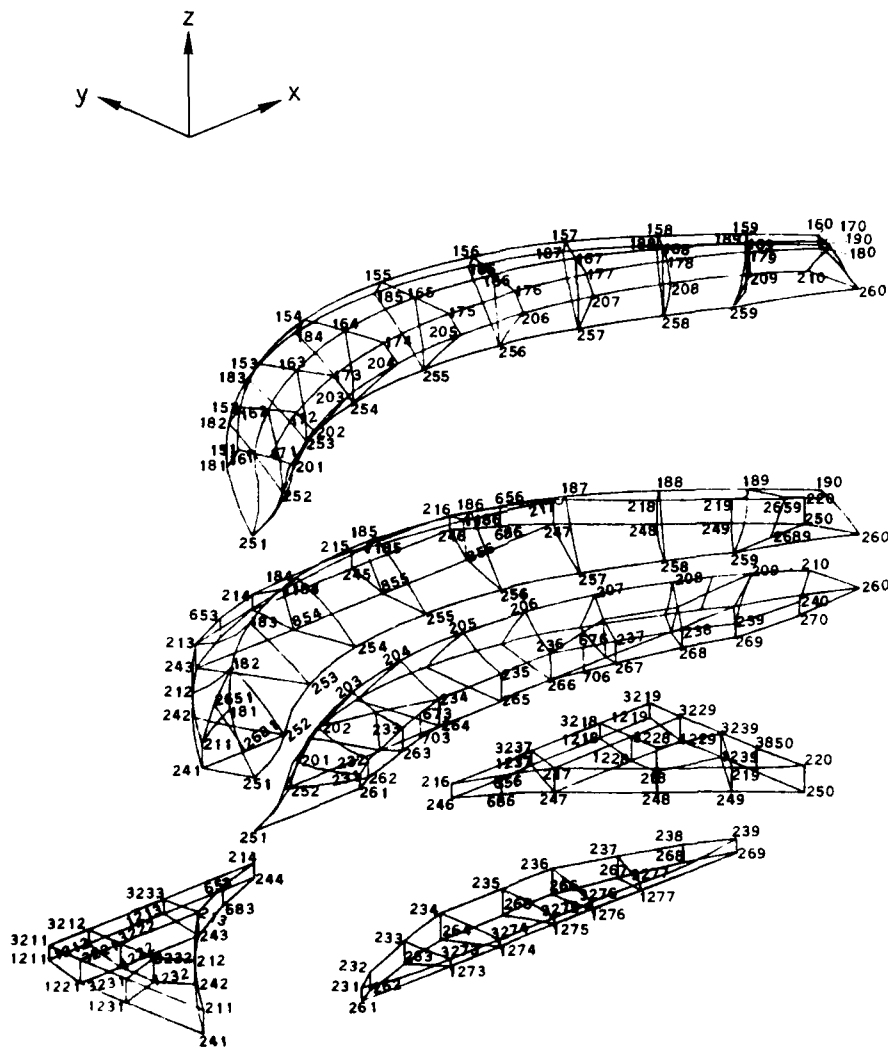


Figure 3.4 Stiffness Data Set 5

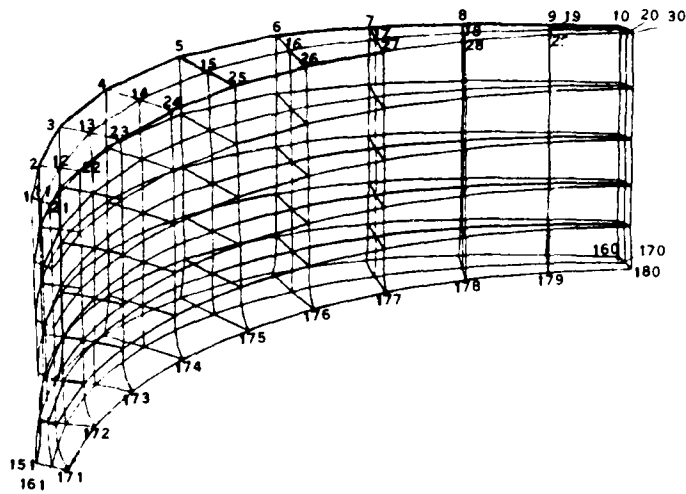
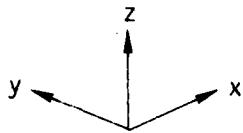


Figure 3.5 Stiffness Data Set 6

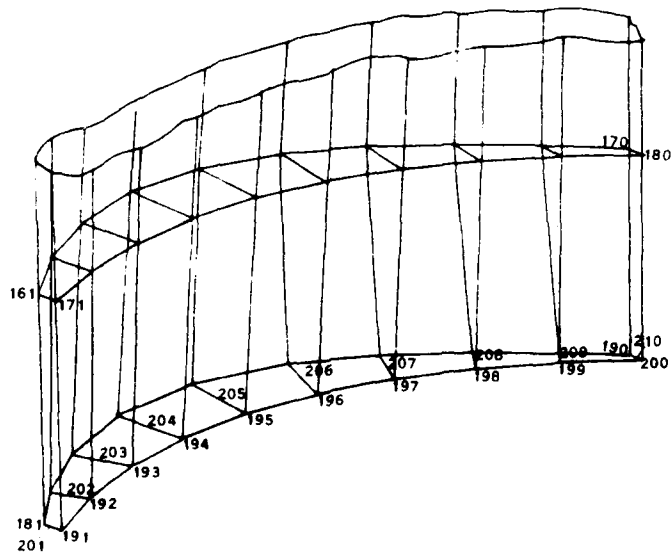
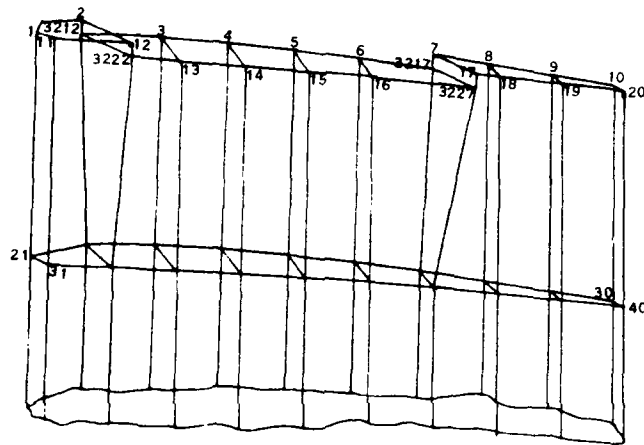
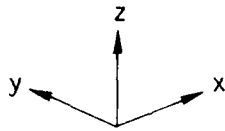


Figure 3.6 Stiffness Data Set 3

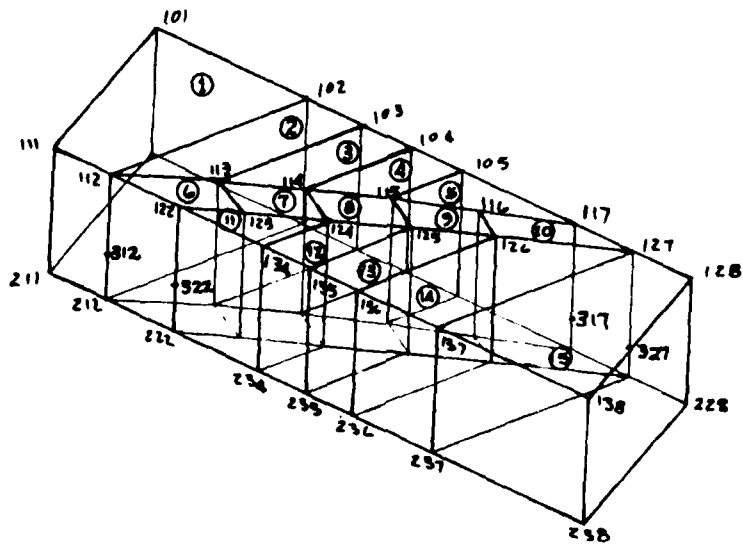
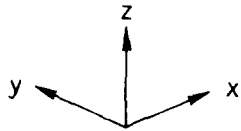


Figure 3.7 Stiffness Data Set 4

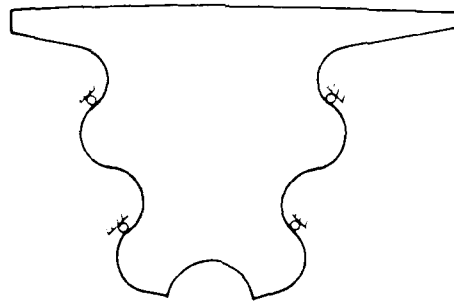
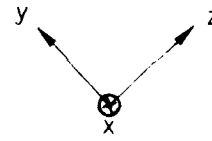
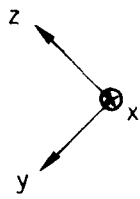


Figure 3.8 Root Boundary Conditions and Coordinate System

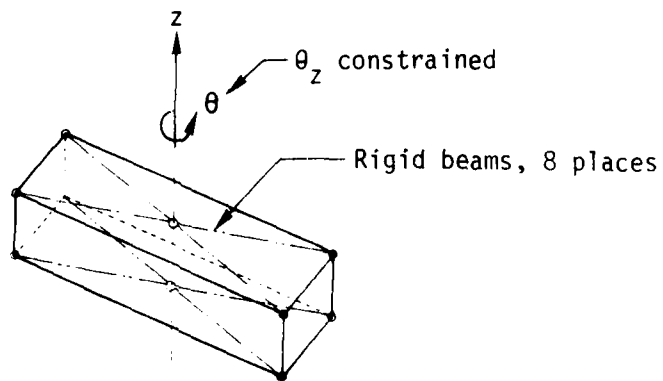


Figure 3.9 Tip Shroud Boundary Condition

J18-47

Four basic loadcases were considered in this analysis. They were centrifugal loads, thermal loads, aerodynamic loads, and a tip rub load. In addition to the basic loadings, various combinations of the basic loads were considered.

Centrifugal loads were generated by an external data generator since the ATLAS inertia loading capability was not operational at the time of this analysis. The loads generated were due to rotation at 16,000 rpm around the global x-axis and were input to the ATLAS system as external nodal forces.

The metal temperatures provided by Lycoming are shown in table 3.2. All temperatures input to the program were interpolated from the Lycoming data by a computer program in order to obtain the necessary accuracy for the fine element mesh.

Table 3.2 Temperature vs. Z-Coordinate

Temperature, F	Z-Coordinate, Inches
1145	4.00
1145	4.95
1145	5.00
1150	5.20
1170	5.70
1192	6.00
1240	6.50
1285	7.00
1323	7.50
1354	8.00
1367	8.50
1362	9.00
1325	9.50

Aerodynamic pressure loads were also provided by Lycoming and are given in table 3.3. Pressure loads were computed as a function of chord length and Z-coordinate and input to the program as element surface pressure loads.

The tip rub load was assumed to be 50 pounds acting in the negative tangential direction at the tip shroud.

D1 4100 7740 ORIG. 3/71



J15-47

Table 3.3 Blade Pressures

Percent Chord	Z=5.13 Inches Pressure, psi	
	Pressure Side	Suction Side
0	17.87	17.87
10	15.11	12.54
20	15.20	12.03
30	15.26	11.95
40	15.26	12.02
50	15.26	12.09
60	15.01	11.99
70	14.90	11.97
80	14.79	12.18
90	14.59	12.78
100	17.87	17.87

Table 3.3 Blade Pressures (Continued)

Percent Chord	Z=7.30 Inches Pressure, psi	
	Pressure Side	Suction Side
0	19.90	19.90
10	18.51	15.37
20	18.44	14.75
30	18.32	13.95
40	17.95	12.68
50	17.71	11.83
60	17.61	11.52
70	17.41	11.75
80	17.01	12.37
90	16.33	13.53
100	19.90	19.90

Table 3.3 Blade Pressures (Concluded)

Percent Chord	Z=9.04 Inches Pressure, psi	
	Pressure Side	Suction Side
0	23.28	23.28
10	19.57	14.31
20	19.19	13.66
30	19.10	12.65
40	19.15	11.74
50	19.03	11.20
60	18.76	10.99
70	18.18	11.36
80	17.41	11.70
90	16.82	12.85
100	23.28	23.28

D1.4100 7740 ORIG. 8/71



4.0 PROGRAM EXECUTION

Execution of a stress analysis using the ATLAS System can be as simple as inputting the words "PERFORM STRESS." However, large three-dimensional analyses will require more user interaction. For those analyses requiring such interaction, ATLAS provides a concise control language that allows step by step management of the solution process. This approach was used extensively in the execution of the demonstration problem.

The solution steps for the demonstration problem were grouped into five logical blocks as follows:

1. Input data
2. Generate stiffness and loads matrices
3. Interact substructures
4. Merge and reduce substructures
5. Back substitute for displacement solutions, calculate stresses and print out nodal point stresses.

The first three blocks were executed for all substructures at once while the last two blocks were executed once for each substructure except substructures 13 and 14 which were executed together. Each of the above blocks utilized one or more ATLAS executive statements.

It was found in the first attempt to execute the problem that the initial substructuring arrangement contained a substructure which produced more data than could be stored on a single disk storage device on the production configuration of the BCS CDC 6600. The job would have aborted due to a track limit error. The offending substructure was broken into two substructures, numbered 15 and 16, and, as a result of this experience, guidelines were set up which reduced the probability of further track limit aborts. These guidelines involved careful data management through the use of substructuring, ATLAS executive statements, and CDC 6600 job control cards, together with a good understanding of the substructure's gross stiffness matrix effective half bandwidth. The guidelines are outlined below.

First, if the length of any one substructure data file such as the stiffness matrix file or merge data file exceeds one-half the capacity of the device on which it is stored, the problem size should be reduced by replacing that substructure with two or more substructures whose data files fit the above criterion.

Second, whenever possible, assign the largest data files to different disk storage devices through CDC 6600 job control cards. For example, restart files such as SAVESF should be



assigned to a different disk than the files being loaded to or from SAVESF such as STIFRNF, etc.

Third, use the ATLAS "SAVE MATRIX" option to separate data files according to when they are needed in the execution process. For example, store the element stiffness matrices and the element stress matrices which are generated at the same time on separate save files so that they may be loaded as needed rather than in one large file.

Execution of the demonstration problem without substructuring would have required up to 40 million words of disk storage space. However, with the use of the guidelines given above, the required disk space was reduced to about 12 million words. The maximum length of a single file was about 3 million words which was well within the 10 million word capacity of a single storage device. Thus, the problem could be executed on the production configuration of the BCS CDC 6600.

The interested reader is referred to the ATLAS control program listings in appendix A for details of data management.

J1A-47

D1 4100 7740 ORIG. 3/71



5.0 STRESS CONTOUR PLOTS

Contour plots of the pressure and suction surface radial stresses were made for stiffness data set 6. Plots for each of the following loadcases are shown in figures 5.1-5.12.

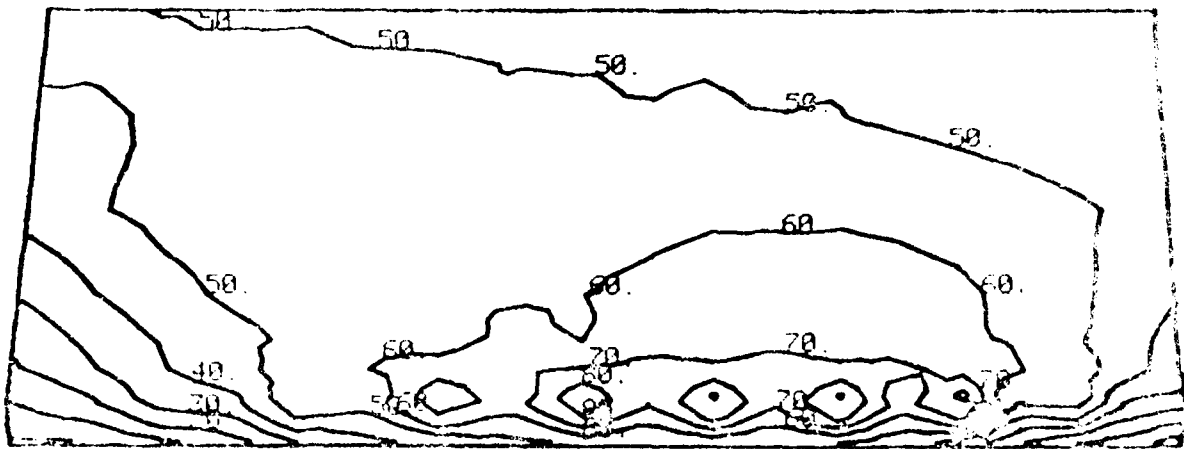
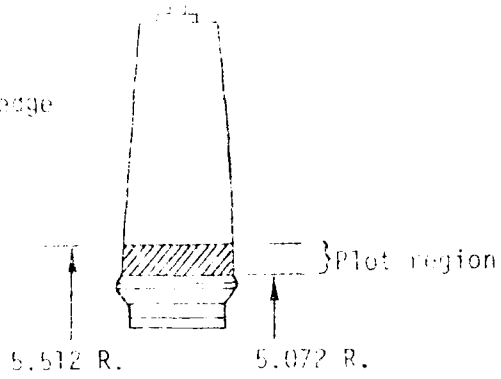
- a) Centrifugal force (fig. 5.1, 5.2)
- b) Aerodynamic loads (fig. 5.3, 5.4)
- c) Thermal loads (fig. 5.5, 5.6)
- d) Tip rub loads (fig. 5.7, 5.8)
- e) Combination of cases a-c (fig. 5.9, 5.10)
- f) Combination of cases a-d (fig. 5.11, 5.12)

The periodic islands that appear in some of the plots are a result of the contour plotting method used. The magnitude of the stresses at the center of those islands is correct, but the adjacent contours are distorted as far as location is concerned and should be judged accordingly.

01 4100 7740 ORIG. 3/71



Leading edge



Stress contours, ksi

Figure 5.1 Radial Stress, CF Load, Pressure Side

REV SYM

REV SYM

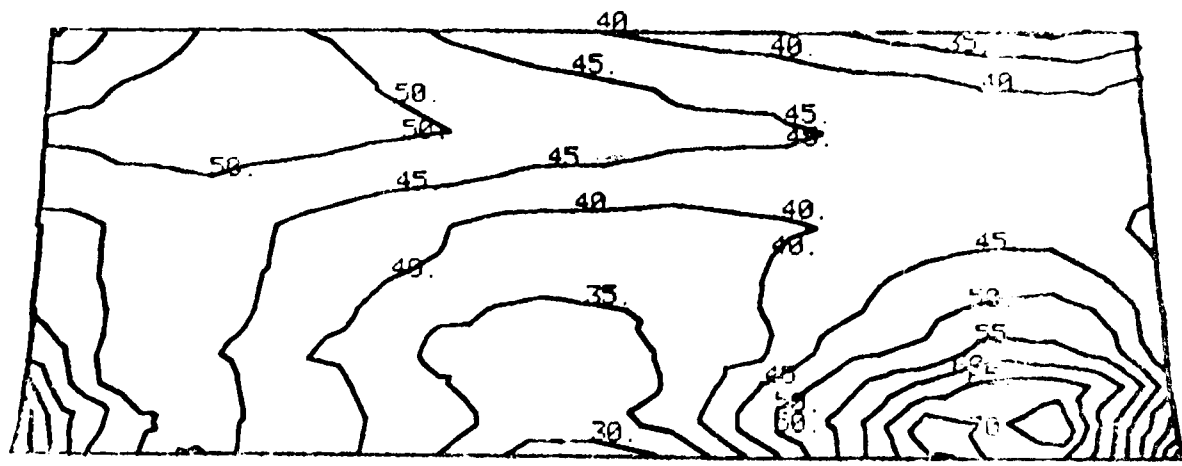
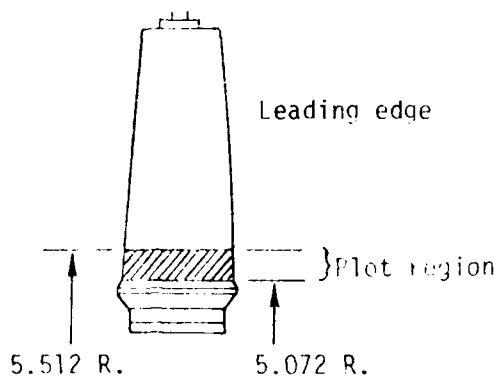
BOEING

NO. 40730

PAGE 20



518747



Stress contours, ksi

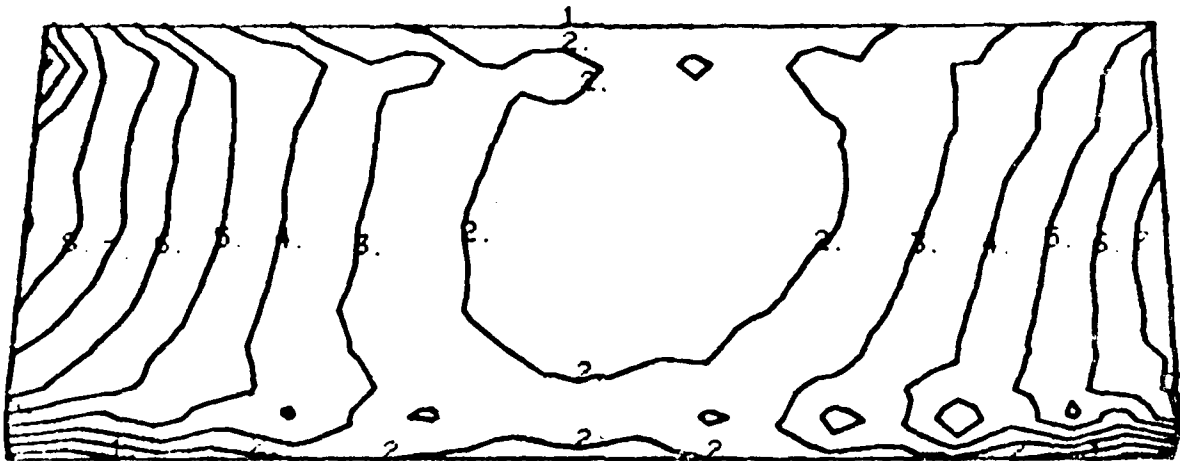
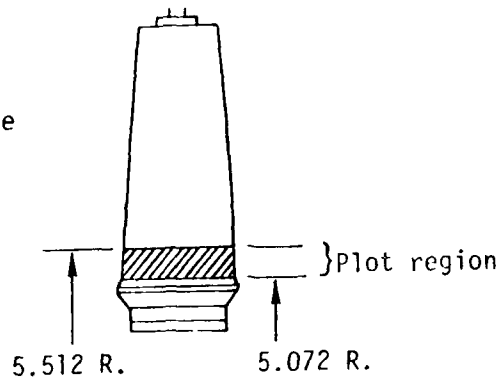
Figure 5.2 Radial Stress, CF Load, Suction Side

214100 7742 OR 5.8771



J18-047

Leading edge



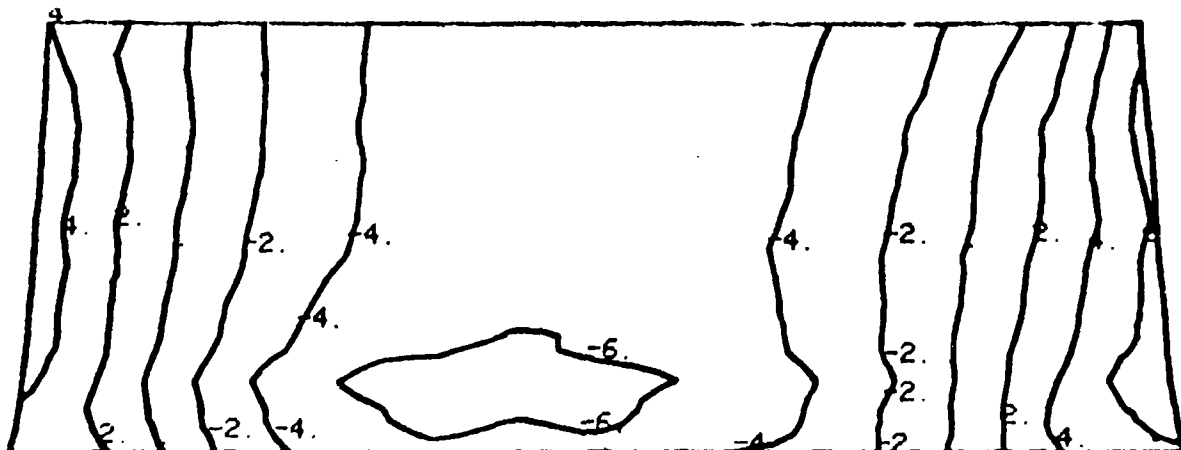
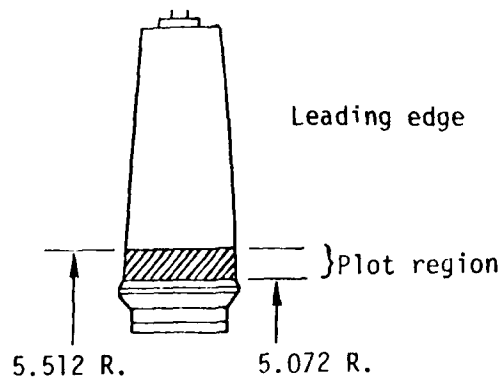
Stress contours, ksi

Figure 5.3 Radial Stress, Aero Load, Pressure Side

D14100 7743 OR 6.3/11



J18-C47



Stress contours, ksi

Figure 5.4 Radial Stress, Aero Load, Suction Side

01 4100 7740 ORIG. 2/71



J18-247

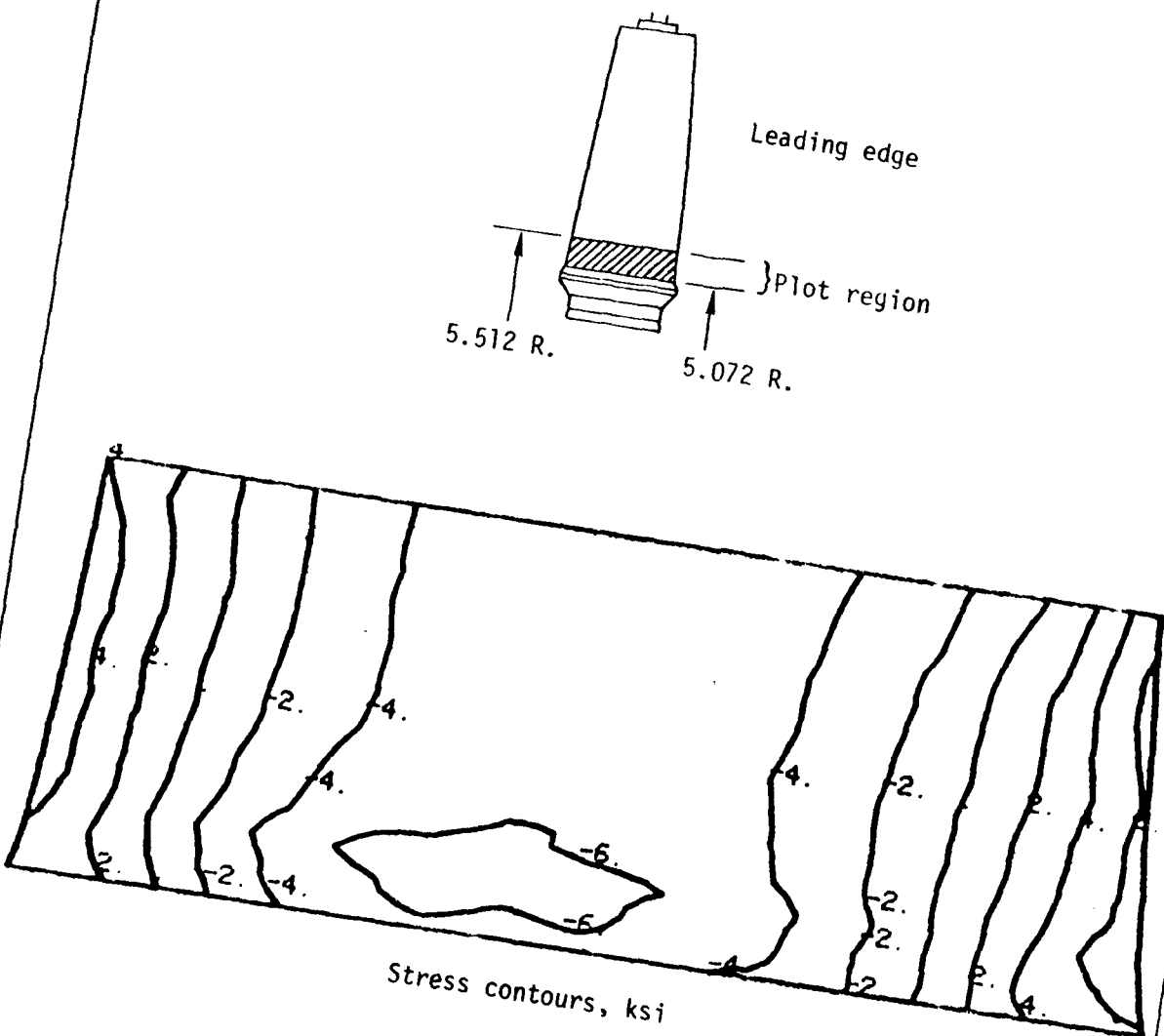
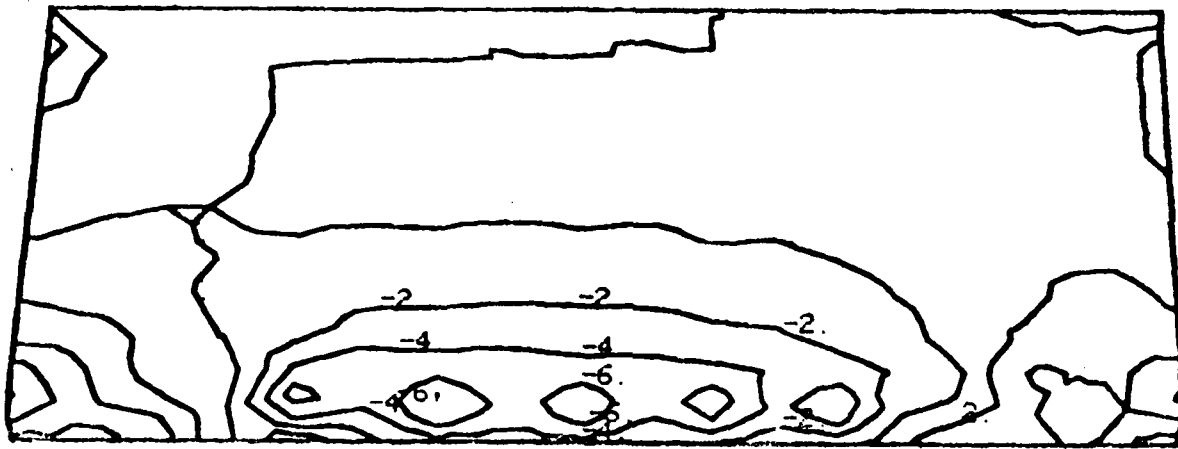
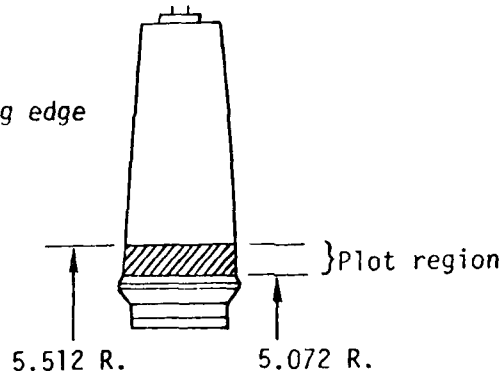


Figure 5.4 Radial Stress, Aero Load, Suction Side

Leading edge

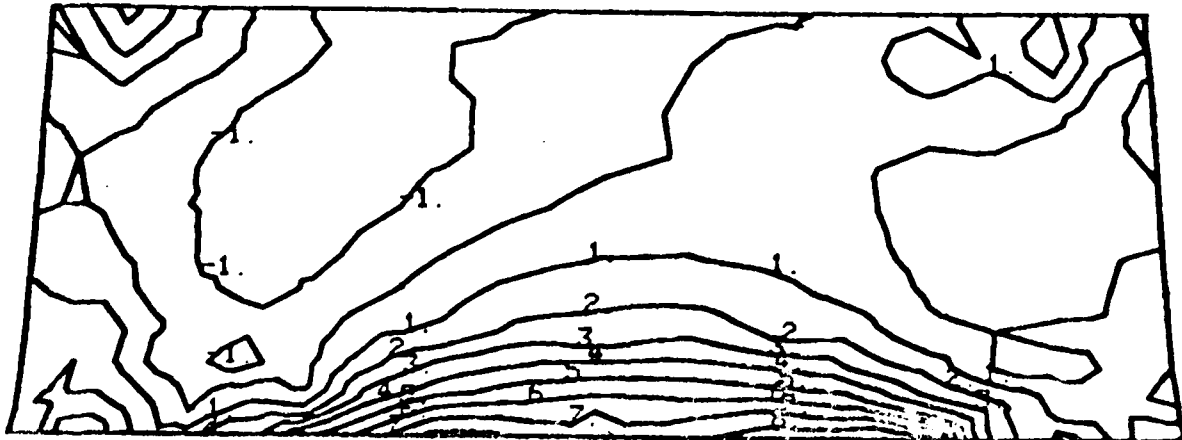
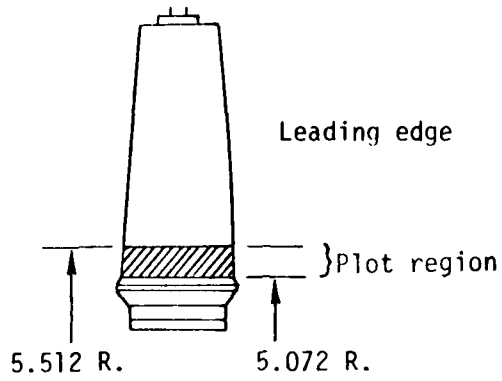


Stress contours, ksi

Figure 5.5 Radial Stress, Thermal Load, Pressure Side



J16-047



Stress contours, ksi

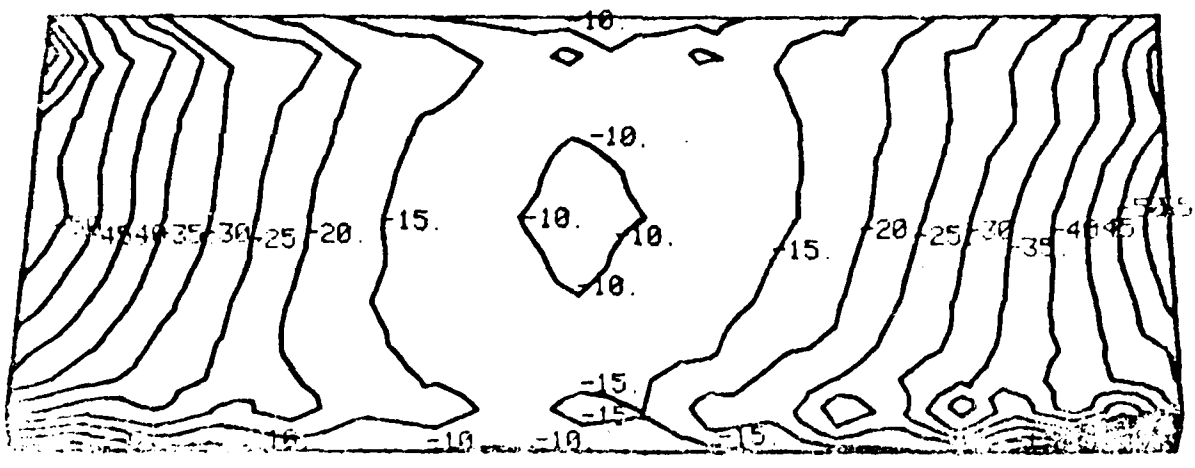
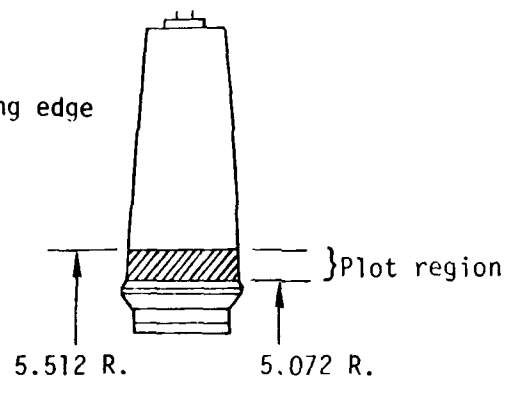
Figure 5.6 Radial Stress, Thermal Load, Suction Side

01 4103 1741 OR 6.3/71



JIF-642

Leading edge



Stress contours, ksi

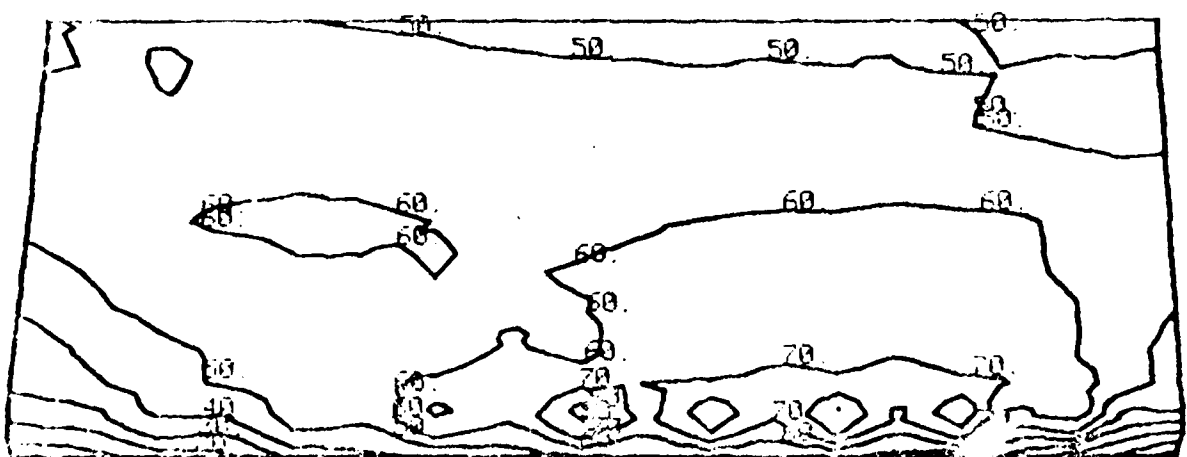
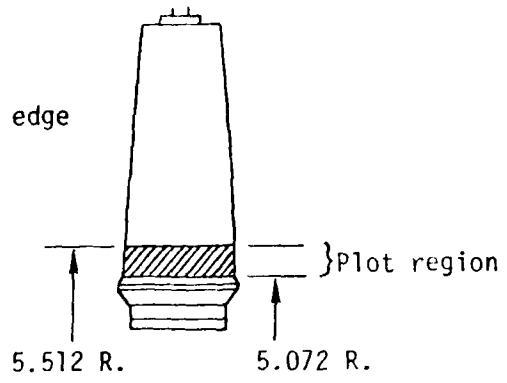
Figure 5.7 Radial Stress, Tip Rub Load, Pressure Side

D1 4100 7740 ORIG. 2/71



J:11-047

Leading edge



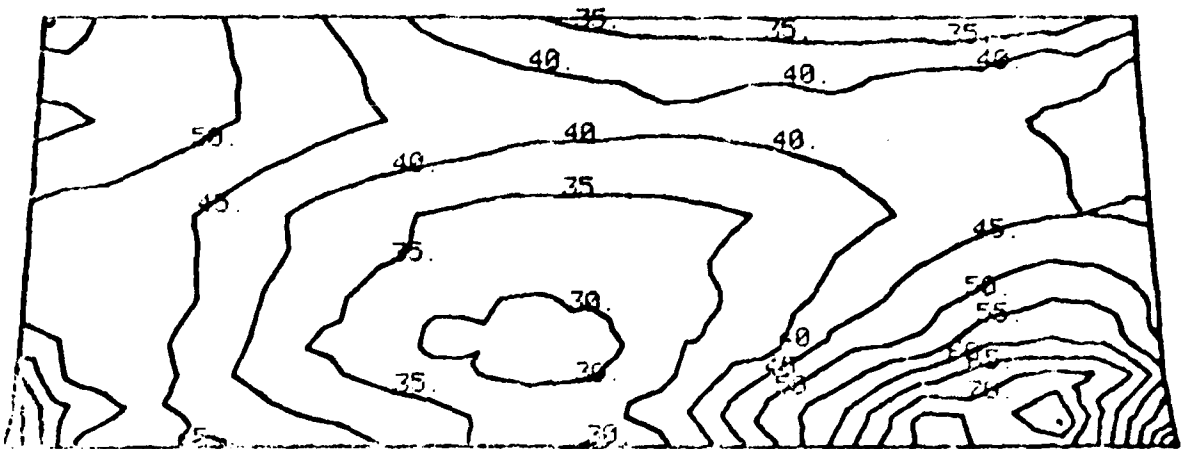
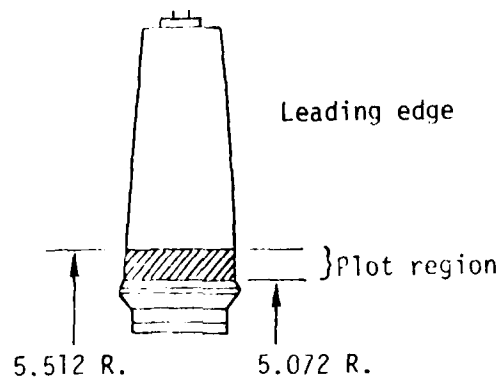
Stress contours, ksi

Figure 5.9 Radial Stress, CF + Aero + Thermal Loads, Pressure Side

D1 4100 7740 OR.G.3/71



018-247



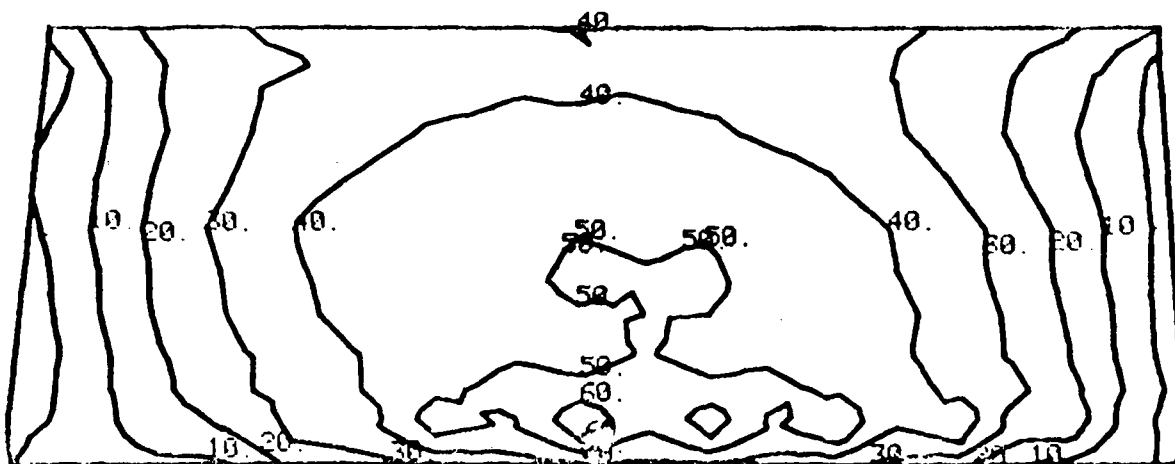
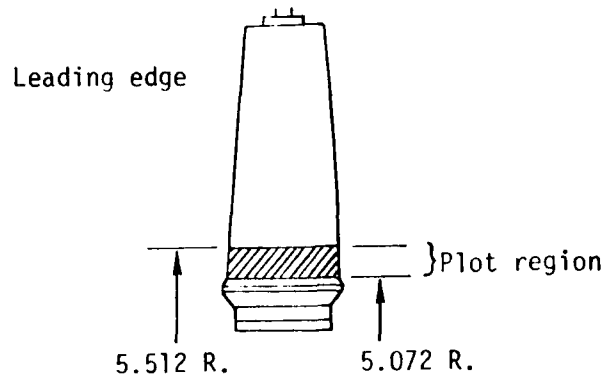
Stress contours, ksi

Figure 5.10 Radial Stress, CF + Aero + Thermal Loads, Suction Side

018-247 09-03/71



515-147



Stress contours, ksi

Figure 5.11 Radial Stress, CF + Aero + Thermal + Rub Loads, Pressure Side



J18-647

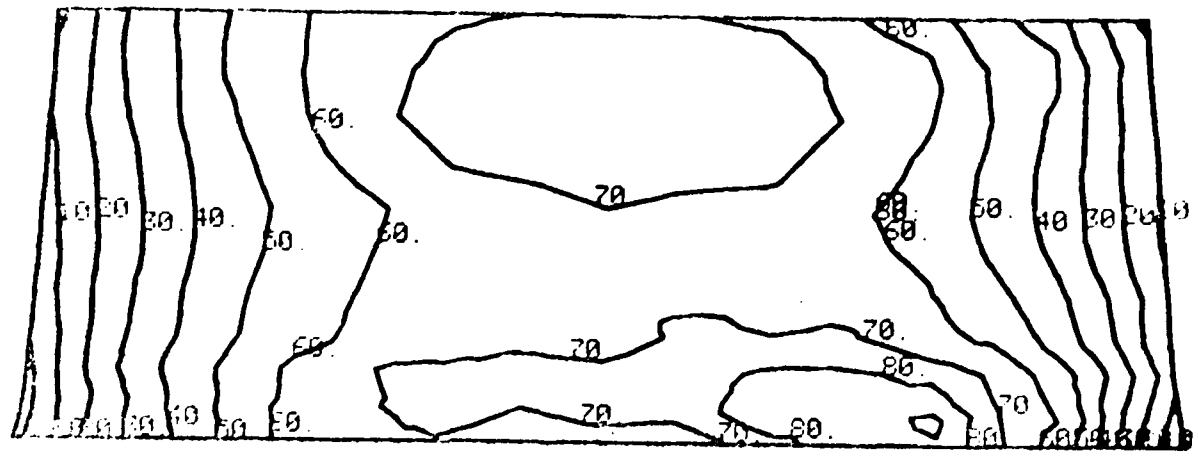
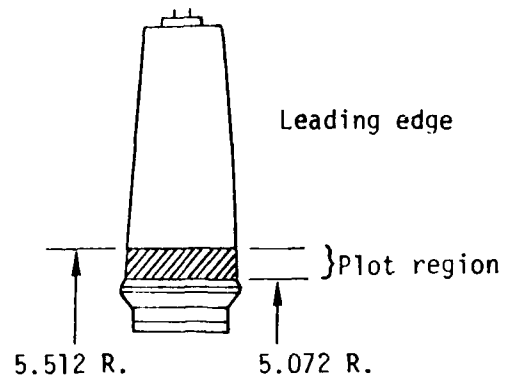


Figure 5.12 Radial Stress, CF + Aero + Thermal + Rub Loads, Suction Side

DI 4100 7740 OR G.3/71



J18-047

6.0 TWO- AND THREE-DIMENSIONAL ANALYSIS COMPARISONS

The subject turbine blade had undergone several earlier analyses including a two-dimensional NASTRAN plate analysis, a three-dimensional ATLAS analysis with force boundary conditions provided from the NASTRAN analysis, and a full scale photoelastic analysis. In addition to the analytical data, Lycoming test experience provided information as to where the blade failed under overspeed conditions. These data are compared in this section.

Boundary conditions for the numerical analyses described above varied widely according to the complexity of the analysis. The NASTRAN plate analysis boundary conditions assumed that the airfoil was rigidly fixed at the root and constrained against rotation at the tip as shown in figure 6.1. The combination analysis using NASTRAN and ATLAS assumed that the fir tree was supported against radial motion at the bottom of the first land of the fir tree and against translations and rotations along the sides of the fir tree as shown in figure 6.2. Note that the effects of the upper portion of the airfoil and tip constraint were generated by NASTRAN as element forces and subsequently input to ATLAS as nodal forces.

Boundary conditions for the photoelastic study were provided by a real hardware disk. Since the disk material was far more rigid than the plastic blade model, the boundary conditions for the photoelastic study should have been very similar to those shown in figure 3.8.

Field experience for failures due to overspeed indicated that the most frequent point of failure was about .15 inch above the blade platform. This location corresponds to a Z-dimension of 5.13 inches and was used as a basis for comparisons of the results of the three analyses mentioned above and the demonstration problem results. Figures 6.3a and 6.3b show the radial stresses due to centrifugal forces predicted by the four methods (at a Z-dimension of 5.13 inches) for the pressure and suction surfaces of the blade respectively.

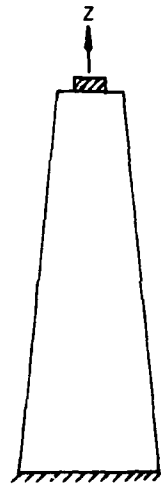
The NASTRAN 2-D analysis predicts average stresses well, but it does not follow the local stress shape displayed by the photoelastic model well. The combination 3-D and 2-D analysis seems to have similar characteristics to the 2-D run only greatly amplified and is the farthest from the photoelastic results. The force boundary condition is thought to be a major contributor to this behavior. The fully 3-D ATLAS analysis has very similar shape characteristics to the photoelastic analysis, although the amplitudes do not match exactly.

The unknowns in the photoelastic study probably outweigh those in the ATLAS analysis. For example, the photoelastic material has a modulus to density ratio of 10^7 while the 713C

01 4100 7740 ORIG. 3/71



J18-047



Tip shroud free to translate -
no rotation about z

Infinitely rigid platform boundary

Figure 6.1 Boundary Conditions for NASTRAN 2-D Analysis

Boundary forces from NASTRAN

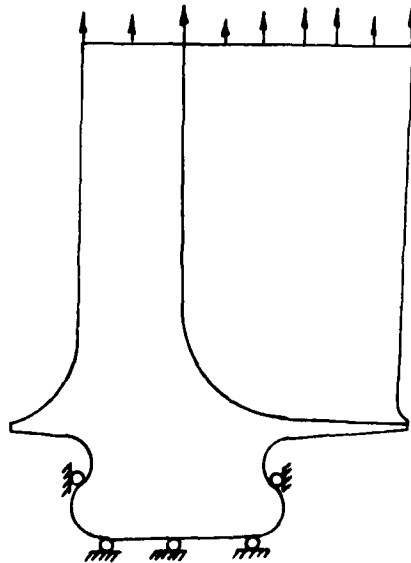


Figure 6.2 Boundary Conditions for ATLAS 3-D + NASTRAN 2-D Analysis

D1 4120 7740 ORIG. 8/71



J18-047

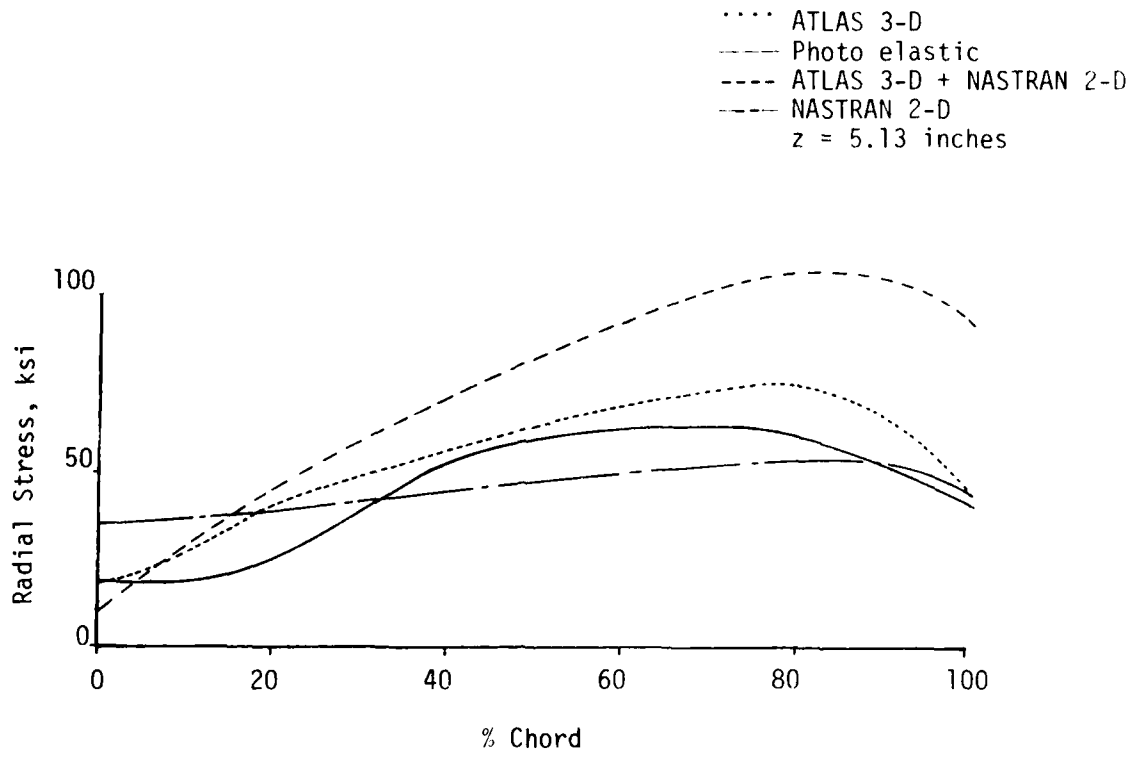


Figure 6.3 (a) Pressure Side Stress Comparison

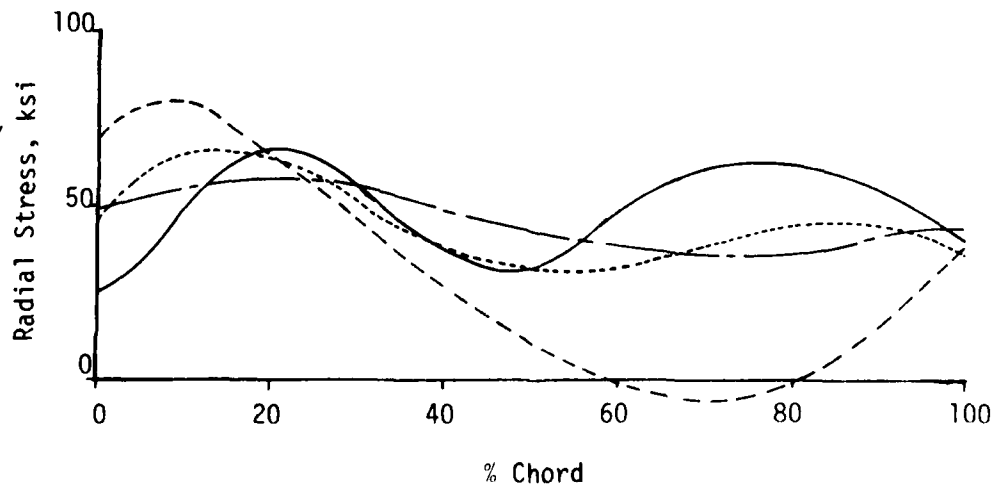


Figure 6.3 (b) Suction Side Stress Comparison

01 4100 7740 ORIG. 3/71



blade material has a ratio of 10^8 . Thus, the nonlinear stiffening effects produced by the centrifugal forces should produce different deflection patterns and different stresses in each model. There is also the possibility that the photoelastic model underwent local yielding at the point of stress concentration which would change the stress picture considerably. It is interesting to note that if yielding had taken place in the region of 60-80% chord on the pressure side of the photoelastic model the stress on the suction side, being below the elastic limit, would have increased due to the transfer of load. If one applies this hypothesis to the ATLAS 3-D data in figure 6.3, the resulting curve shapes would be nearly identical to the photoelastic curves.

A comparison of the ATLAS 3-D, the photoelastic, and test experience data is shown in figure 6.4. Assuming that the overspeed failures were due to centrifugal force overload exclusively, the ATLAS 3-D analysis comes much closer to predicting the failure point than the photoelastic study.

It would appear from the results of these comparisons and other related experience with the three-dimensional isoparametric elements that they provide the most accurate and most versatile three-dimensional method of stress analysis available. The analysis of any geometry should be feasible through the use of substructuring, and the accuracy of the results should be limited only by the analyst's ingenuity and experience and the computer resources available.

DI 4100 7740 ORIG. 3/71



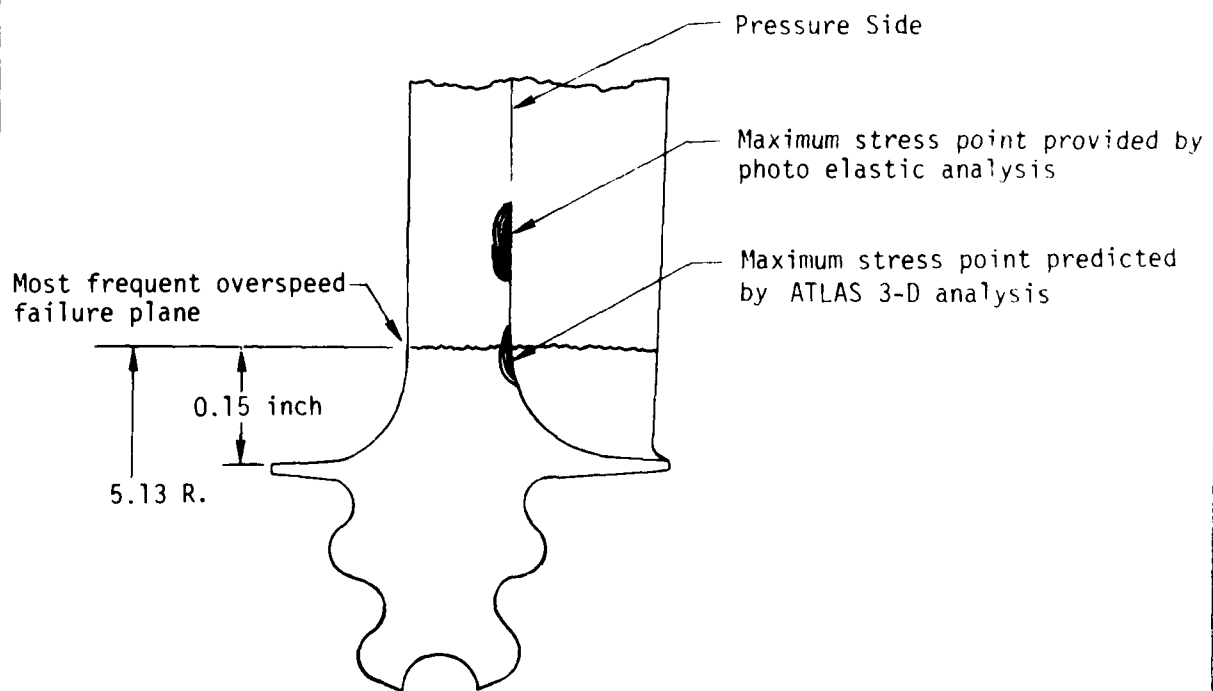


Figure 6.4 Predicted Maximum Stress vs Failure Point Comparison

7.0 CONCLUSIONS AND RECOMMENDATIONS

The following conclusions are a result of this study:

1. ATLAS provides an accurate three-dimensional elastic stress analysis capability for analyzing complex structures such as turbine blades.
2. Efficient management of very large volumes of data is as important to successful 3-D analysis as the element itself.
3. Substructuring is essential to three-dimensional analysis of complex structures such as turbine blades and disks.

The following are recommended areas for further study:

1. A nonlinear analysis using an iterative displacement and/or differential stiffness approach should be made to determine the effect of centrifugal stiffening on local stresses.
2. Plastic analyses through the use of substructuring and piecewise linear analysis should be explored.
3. Known stress concentrators such as fillets should be modeled with different order bricks and results tabulated. This could be accomplished by modeling the concentrator configurations documented by Roark (ref. 3) or Peterson (ref. 4).
4. Boundary condition options which allow tensile or compressive reactions but not both should be tried in modeling fir trees in order to study the effects of loss of contact along the lands.



REFERENCES

1. Zienkiewicz, O. C., "The Finite Element Method in Engineering Science," McGraw-Hill, New York, 1971.
2. ATLAS--An Integrated Structural Analysis and Design System, "User's Manual--Input and Execution Data," Boeing Document D6-25400-0003TN, 1974.
3. Roark, R. J., "Formulas for Stress and Strain," 4th Edition, McGraw-Hill Book Company, New York, 1965.
4. Peterson, R. E., "Stress Concentration Design Factors," John Wiley & Sons, Inc., New York, 1953.



APPENDIX A--ATLAS OUTPUT

This appendix contains a complete listing of the ATLAS execution of the demonstration problem. It is intended to provide detailed information for those wishing to carry on further studies of the demonstration blade and to provide a general guide for anyone intending to do three-dimensional stress analysis using the ATLAS system.

The microfiche file at the end of this appendix is organized in blocks according to the ATLAS executive modules used, and corresponds to the following outline:

- A.1 Read input
- A.2 Execution of STIFFNESS and LOADS modules and printing of stiffness data
- A.3 Execution of INTERACT preprocessor and printing of interact data
- A.4 Execution of SS-MERGE and SS-REDUCE procedures to perform matrix merge and reduce operations, and SS-PARTITION procedure to partition the highest level substructure
- A.5 Execution of SS-BACK procedures and STRESS and OUTPUT modules and the nodal stress output routine

Program execution times and computer resource units are given in table A.1 for the major blocks.

D 1 4 100 7740 ORIG. 3/71



11-4

Table A.1 Computation Time and Resources*

Procedure	Substructure Number			
	11	CRUs	13,14	CRUs
CF Loads	Time, sec	54	Time, sec	22
Stiffness/Loads	1696	278	89	25
Merge/Reduce	3673	998	85	29
Backsub/Stress	973	254	220	63
Totals	6342	1584	384	139

Table A.1 Computation Time and Resources* (Continued)

Procedure	Substructure Number			
	15	CRUs	16	CRUs
CF Loads	Time, sec	46	Time, sec	46
Stiffness/Loads	1149	192	1551	254
Merge/Reduce	6667	2026	3034	778
Backsub/Stress	761	214	854	199
Totals	8577	2478	5439	1277

Table A.1 Computation Time and Resources* (Concluded)

Procedure	Substructure Number	
	21	CRUs
Merge/Reduce/Partition	Time, sec	156
	802	

Problem Totals - 21554 seconds and 5634 CRU's.

*Dollar costs are directly proportional to computer resource units.

The total input card count for the demonstration problem was approximately 10,900 cards.

D1 4100 7740 ORIG. 3/71



A.1	Input		Appendix	D6-42735	1
A.1	Input (Continued)		Appendix	D6-42735	4
A.2	Stiffness and Loads -- SS 11		Appendix	D6-42735	6
A.2	Stiffness and Loads -- SS 13, 14		Appendix	D6-42735	7
A.2	Stiffness and Loads -- SS 15		Appendix	D6-42735	8
A.2	Stiffness and Loads -- SS 16		Appendix	D6-42735	9
A.3	Interact		Appendix	D6-42735	10
A.3	Interact' (Continued)		Appendix	D6-42735	11
A.3	Interact (Continued)		Appendix	D6-42735	12
A.4	Merge and Reduce	SS 11	Appendix	D6-42735	13
A.4	Merge and Reduce	SS 13, 14	Appendix	D6-42735	14
A.4	Merge and Reduce	SS 15	Appendix	D6-42735	15
A.4	Merge and Reduce	SS 16	Appendix	D6-42735	17
A.4	Merge and Reduce	SS 21	Appendix	D6-42735	18

A.5	Back Sub/Stress/Output	SS 11	Appendix	D6-42735	19
A.5	Back Sub/Stress/Output	SS 11	Appendix	D6-42735	22
A.5	Back Sub/Stress/Output	SS 11	Appendix	D6-42735	24
A.5	Back Sub/Stress/Output	SS 11	Appendix	D6-42735	25
A.5	Back Sub/Stress/Output	SS 13, 14	Appendix	D6-42735	28
A.5	Back Sub/Stress/Output	SS 13, 14	Appendix	D6-42735	30
A.5	Back Sub/Stress/Output	SS 15	Appendix	D6-42735	31
A.5	Back Sub/Stress/Output	SS 15	Appendix	D6-42735	33
A.5	Back Sub/Stress/Output	SS 15	Appendix	D6-42735	35
A.5	Back Sub/Stress/Output	SS 15	Appendix	D6-42735	36
A.5	Back Sub/Stress/Output	SS 16	Appendix	D6-42735	38
A.5	Back Sub/Stress/Output	SS 16	Appendix	D6-42735	40
A.5	Back Sub/Stress/Output	SS 16	Appendix	D6-42735	42
A.5	Back Sub/Stress/Output	SS 16	Appendix	D6-42735	44

JIR-147

APPENDIX B--STRESS CONTOUR PLOTS

This appendix contains Mises-Hencky equivalent stress contour plots for stiffness data sets 3 and 6. They are recorded for both pressure and suction surfaces of the blade for the following loadcases:

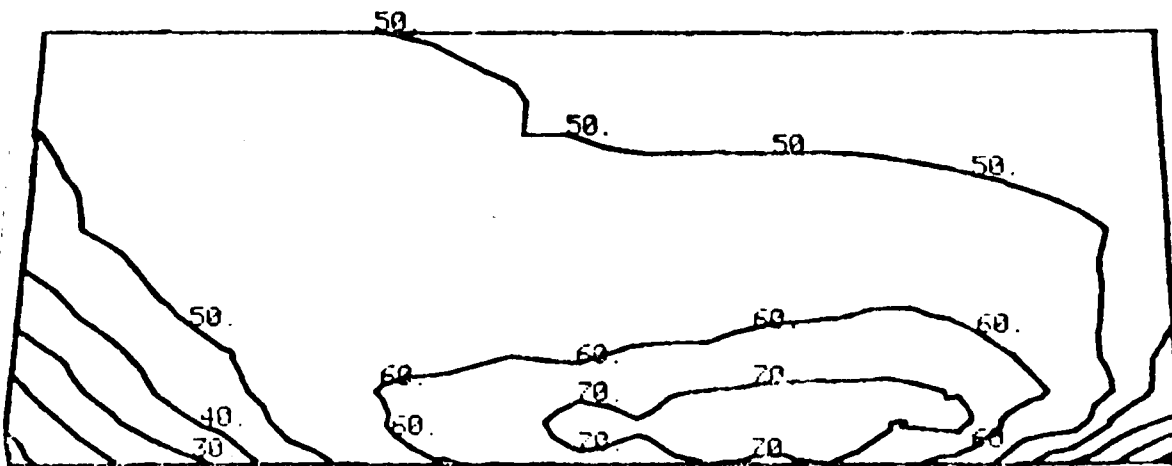
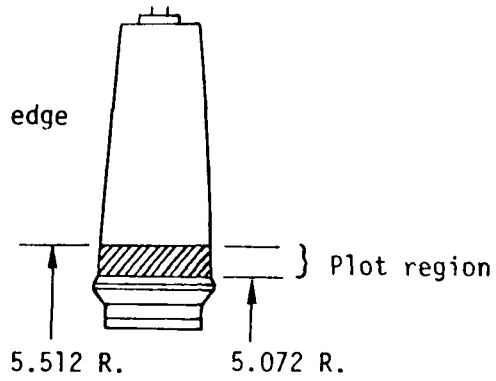
- a) Centrifugal force
- b) Aerodynamic loads
- c) Thermal loads
- d) Tip rub loads
- e) Combination of cases a-c
- f) Combination of cases a-d

D: 4100 7740 ORIG. 2771



J18-247

Leading edge



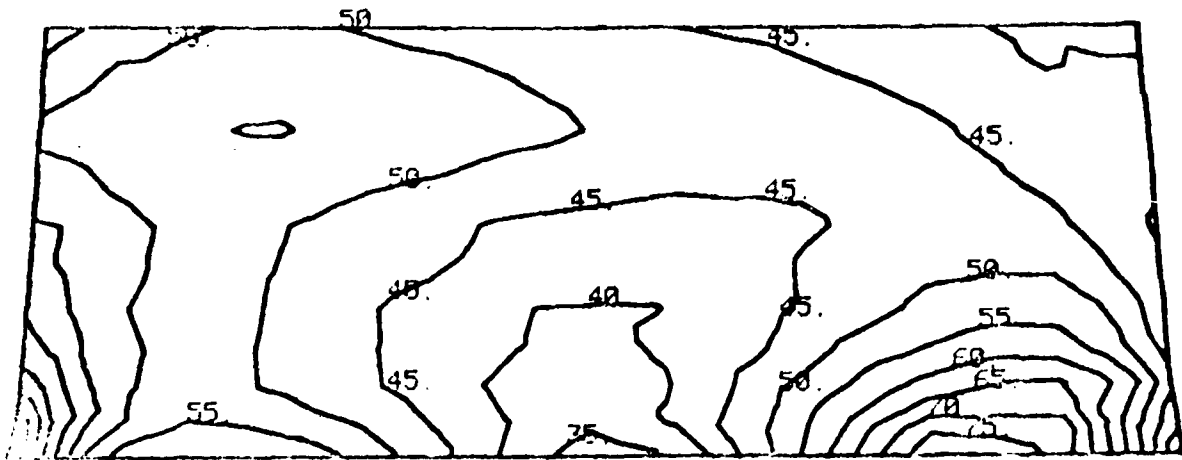
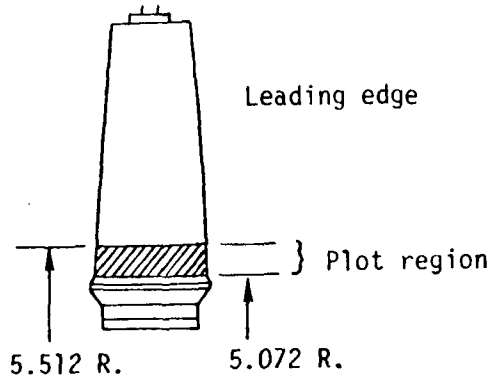
Stress contours, ksi

Figure B.1 Equivalent Stress, CF Load, Pressure Side, Set 6

D14122 774-ORIG.3/71



J. B. 687



Stress contours, ksi

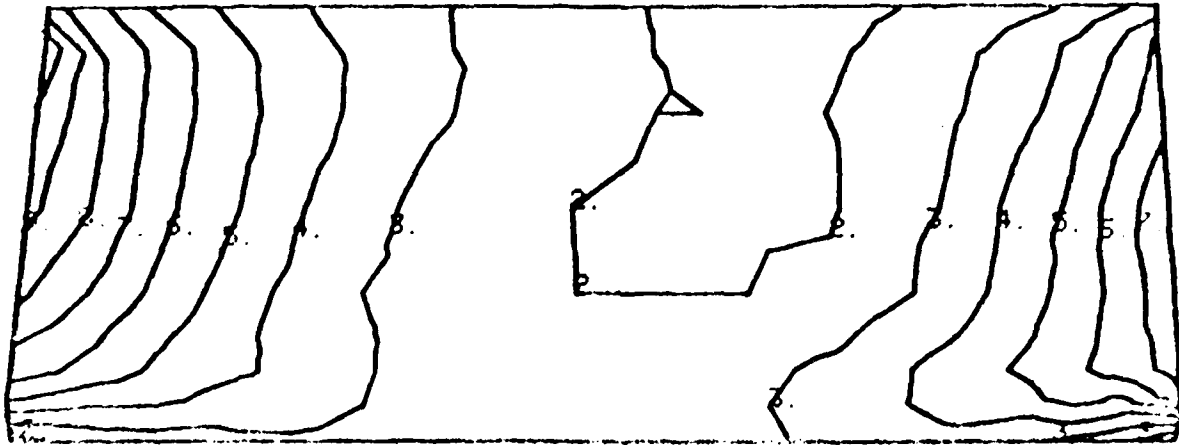
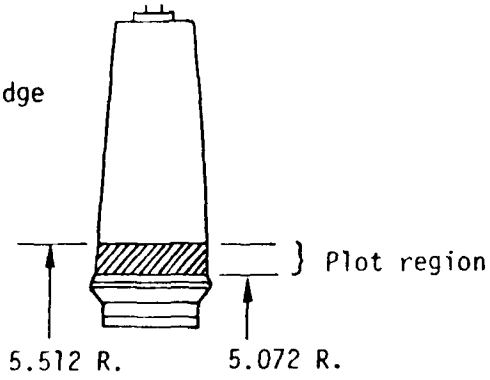
Figure B.2 Equivalent Stress, CF Load, Suction Side, Set 6

D6-4130 7743 CRIG. 3/77



11-47

Leading edge



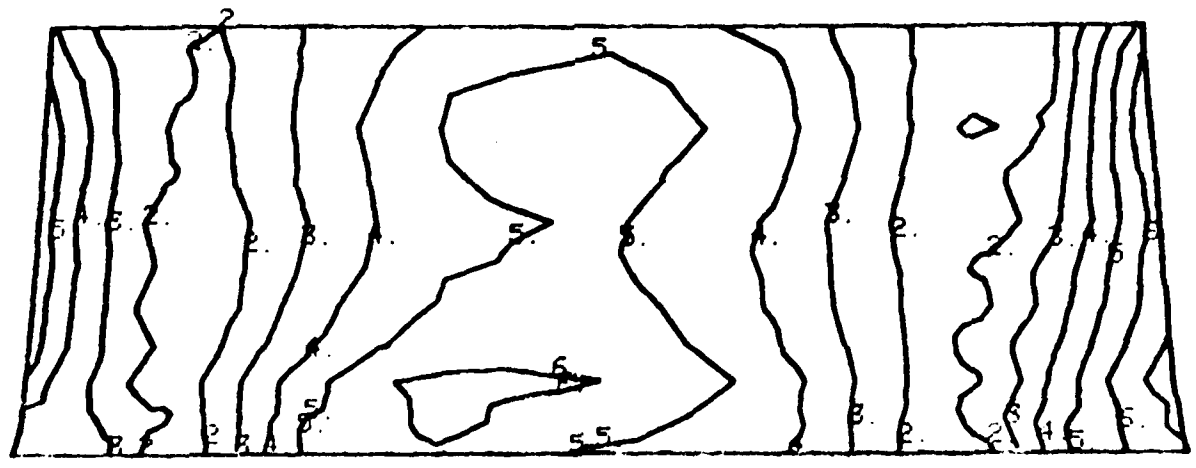
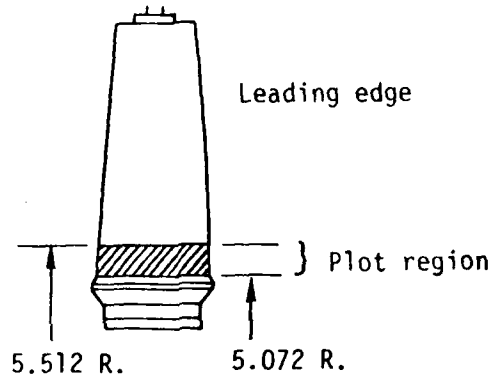
Stress contours, ksi

Figure B.3 Equivalent Stress, Aero Load, Pressure Side, Set 6

11-47



J18-C47



Stress contours, ksi

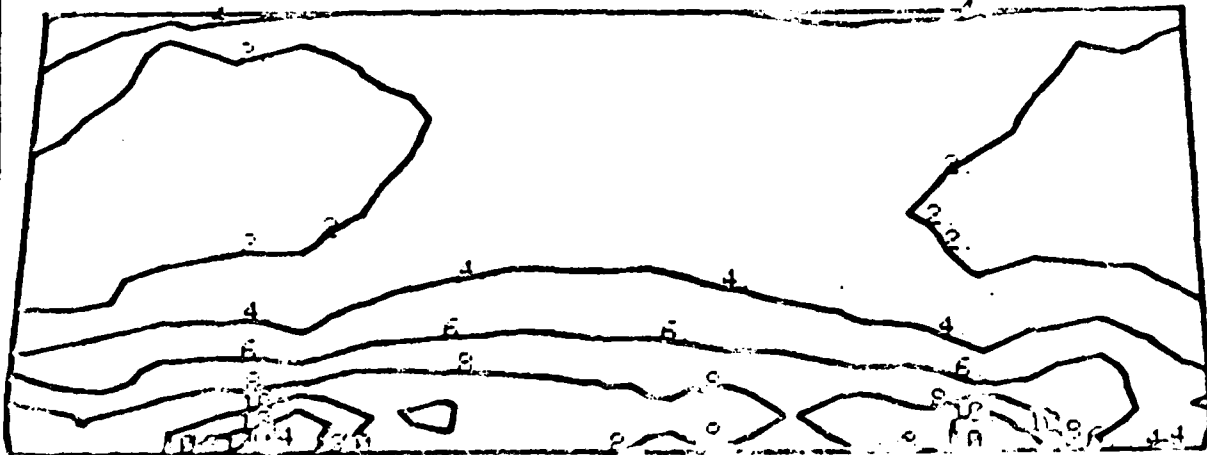
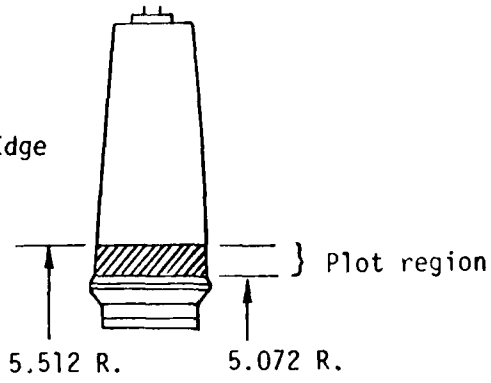
Figure B.4 Equivalent Stress, Aero Load, Suction Side, Set 6

D-4122 7740 OR G.2/71



J15-047

Leading Edge



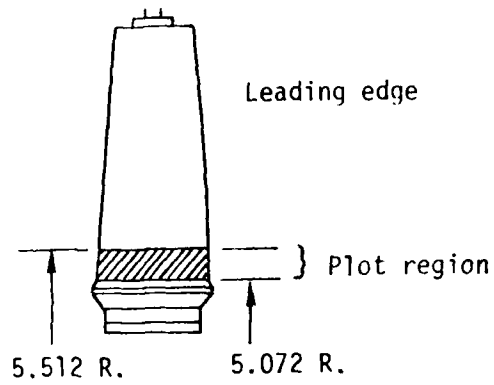
Stress contours, ksi

Figure B.5 Equivalent Stress, Thermal Load, Pressure Side, Set 6

01 4100 7740 ORIG. 3/71



318-143

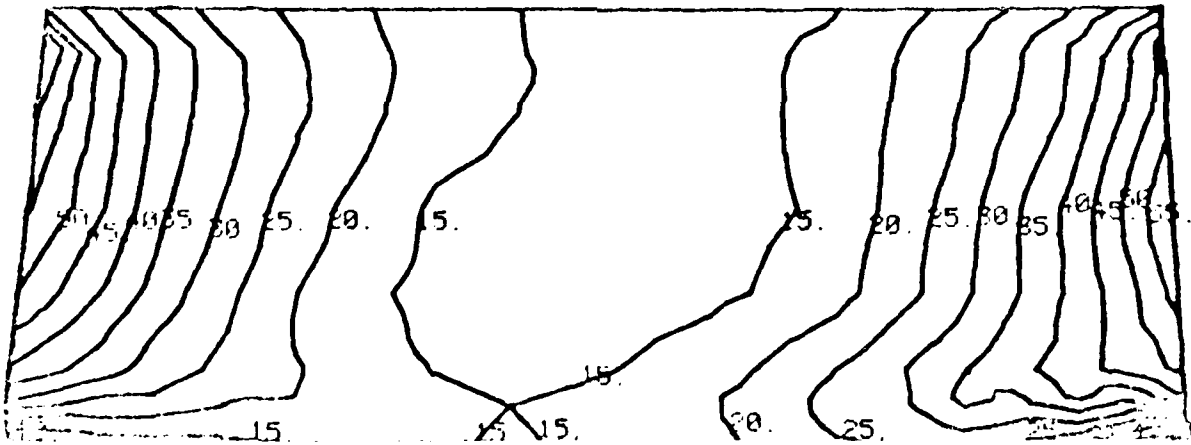
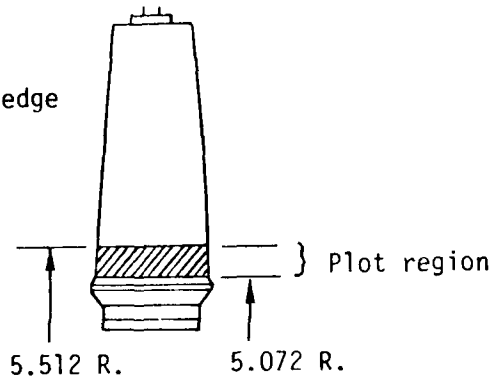


Stress contours, ksi

Figure B.6 Equivalent Stress, Thermal Load, Suction Side, Set 6



Leading edge

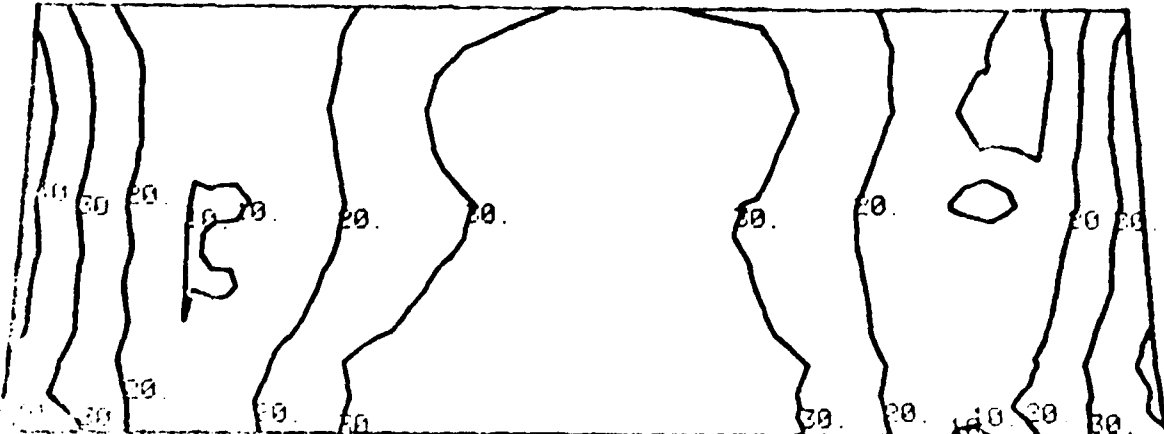
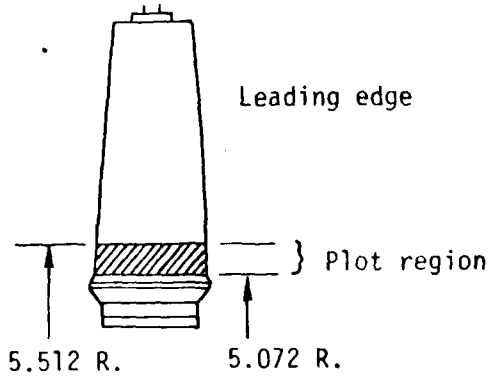


Stress contours, ksi

Figure B.7 Equivalent Stress, Tip Rub Load, Pressure Side, Set 6



11-47



Stress contours, ksi

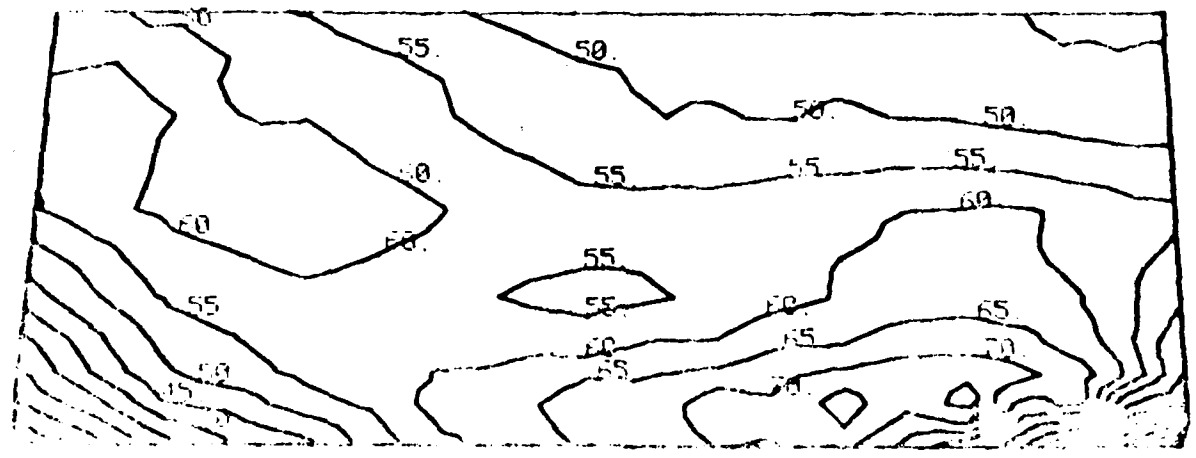
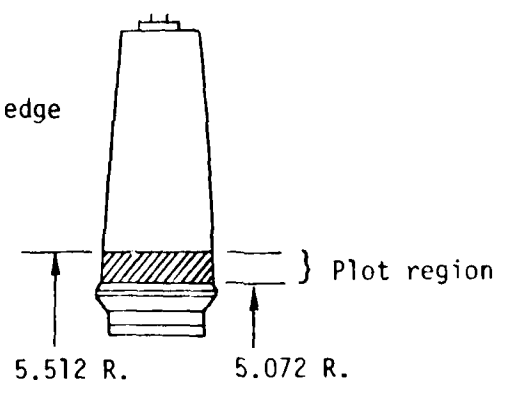
Figure B.8 Equivalent Stress, Tip Rub Load, Suction Side, Set 6

STATO-TAC OR G.371



J10-747

Leading edge



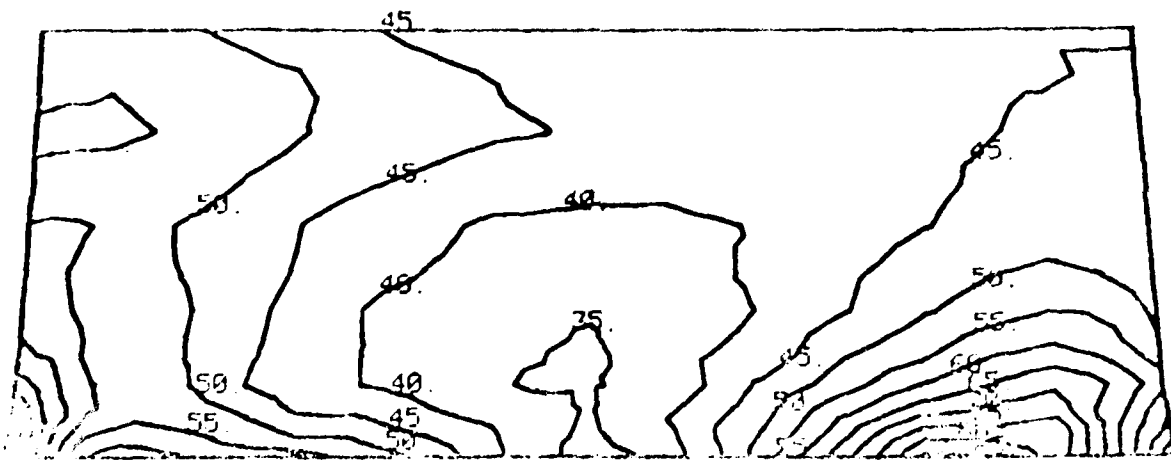
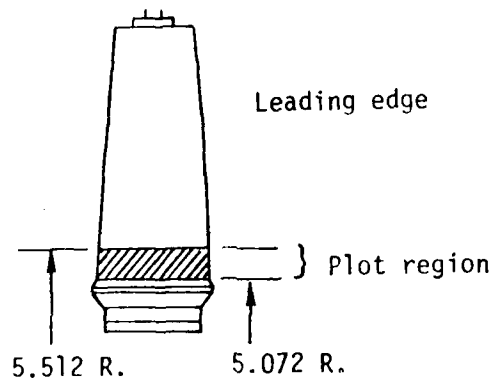
Stress contours, ksi

Figure B.9 Equivalent Stress, CF + Thermal + Aero Loads, Pressure Side, Set 6

S. 415-774L OR G.377



JTB-G47



Stress contours, ksi

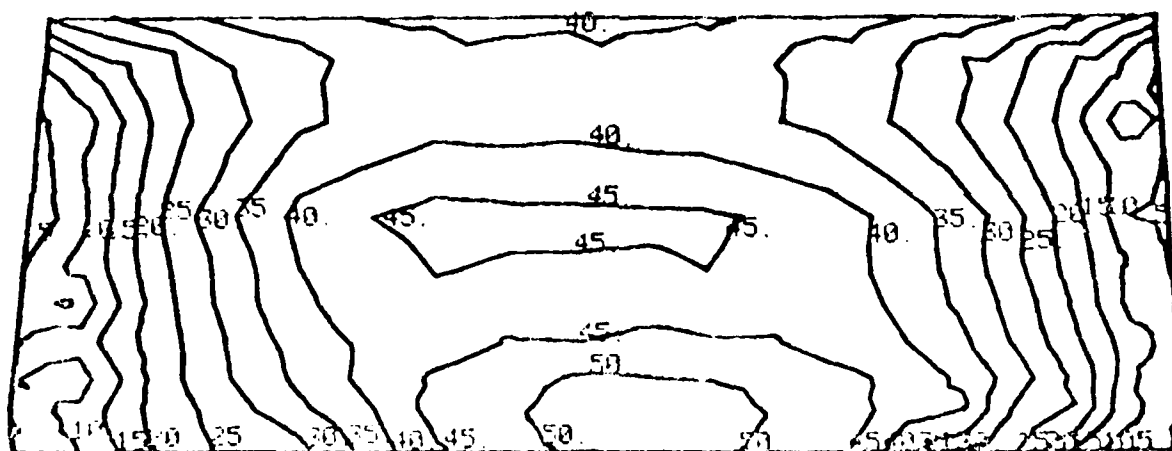
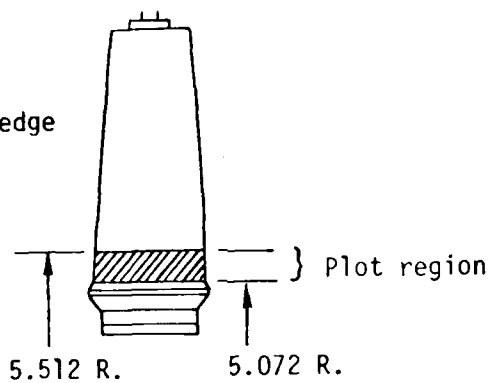
Figure B.10 Equivalent Stress, CF + Thermal + Aero Loads, Suction Side, Set 6

D14111 7740 ORIG. 3/77



J.18-047

Leading edge



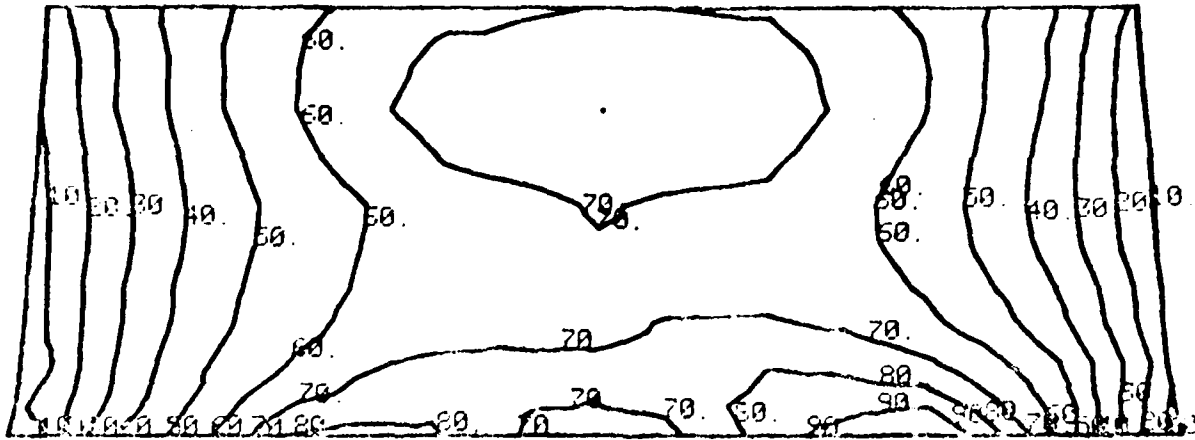
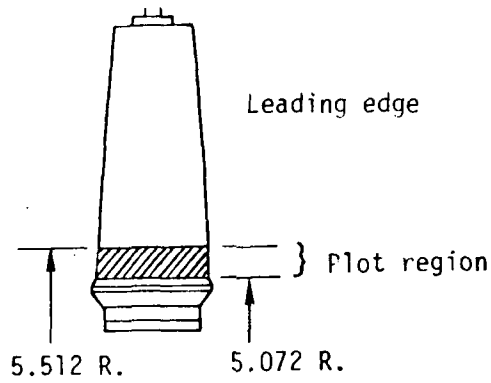
Stress contours, ksi

SI.4. 7740 OR G.3/71

Figure B.11 Equivalent Stress, CF + Aero + Thermal + Rub Loads, Pressure Side, Set 6



014100 7743 OR.G.2/71



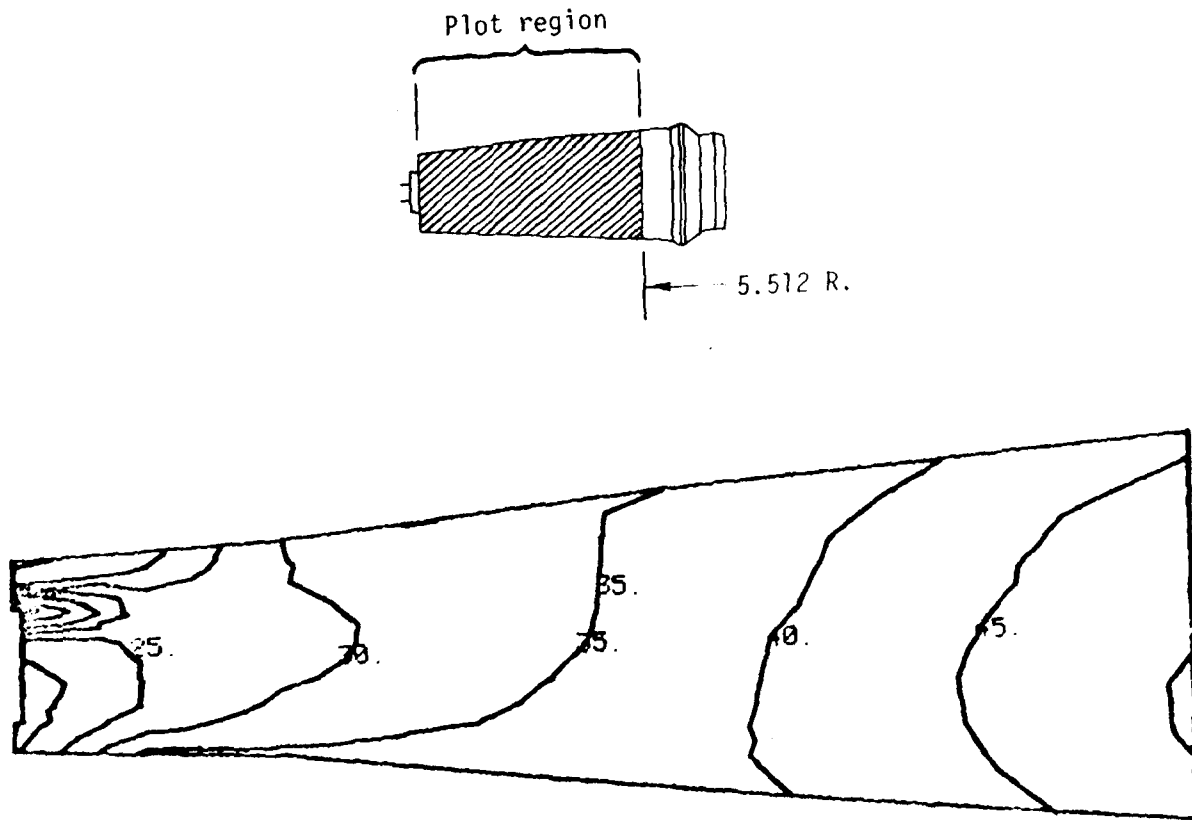
Stress contours, ksi

Figure B.12 Equivalent Stress, CF + Aero + Thermal + Rub Loads, Suction Side, Set 6

014100 7743 OR.G.2/71



J18-047



Leading edge
Stress contours, ksi

Figure B.13 Equivalent Stress, CF Load, Pressure Side, Set 3

D1 4-100 7740 OR. G. 3/71

REV SYM

BOEING

NO D6-42735
PAGE 56



J18-C47

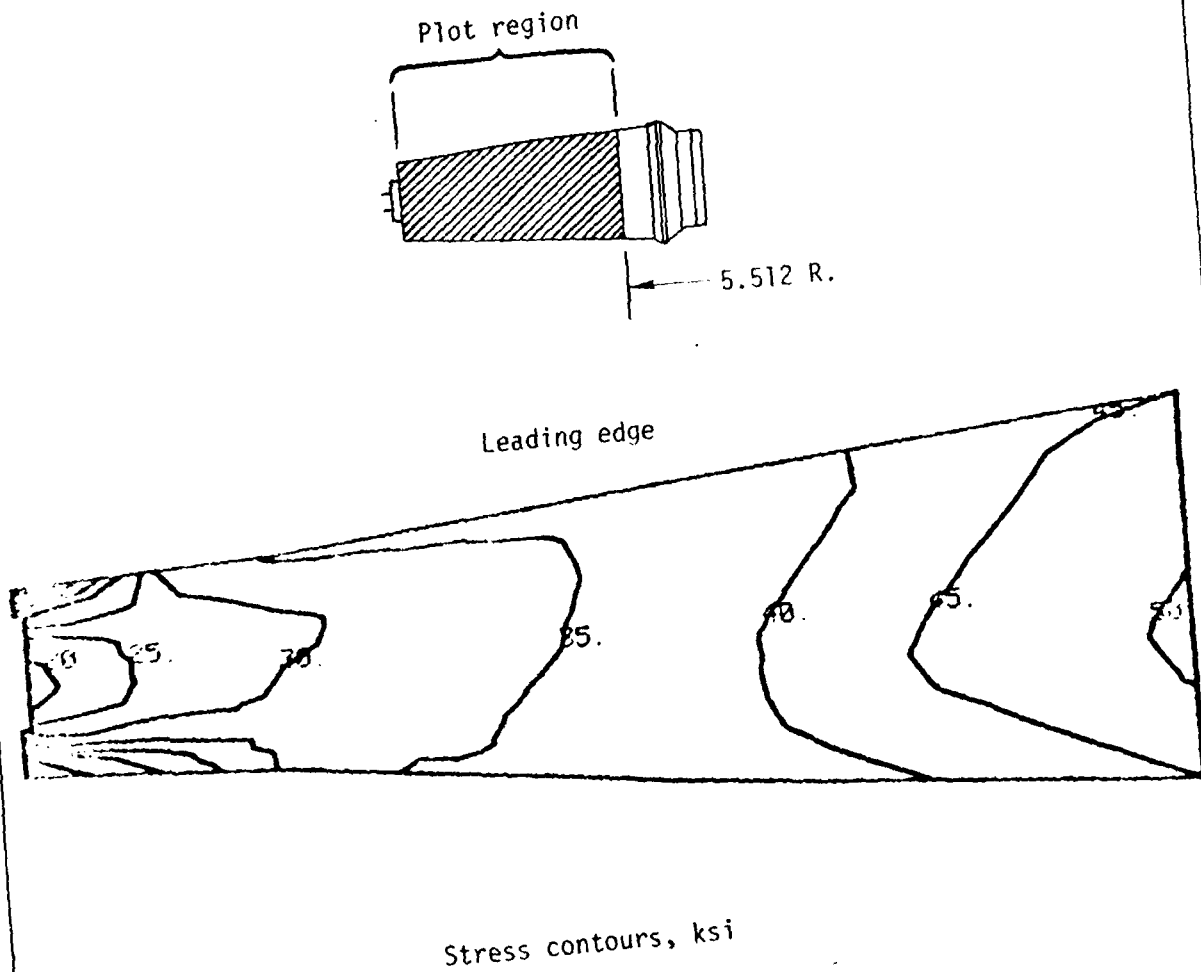


Figure B.14 Equivalent Stress, CF Load, Suction Side, Set 3

D. 4.120 774C OR G. 2/71

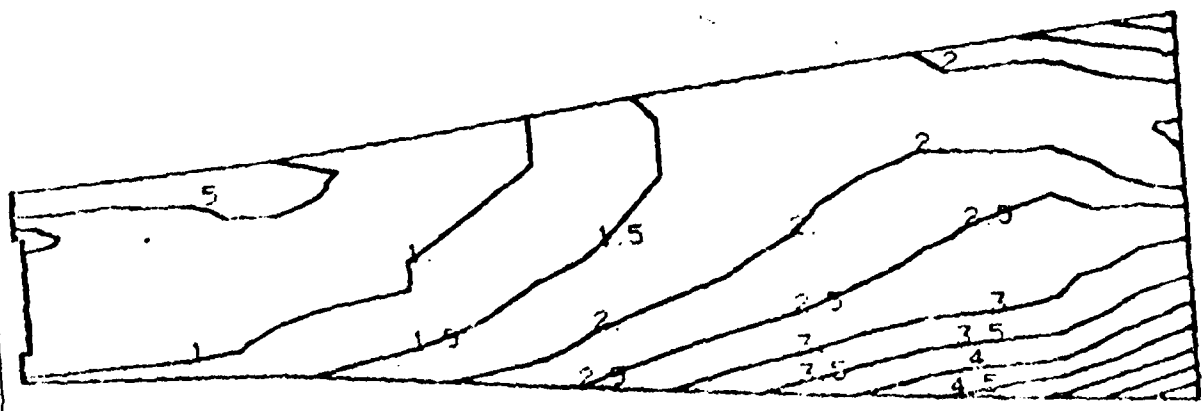
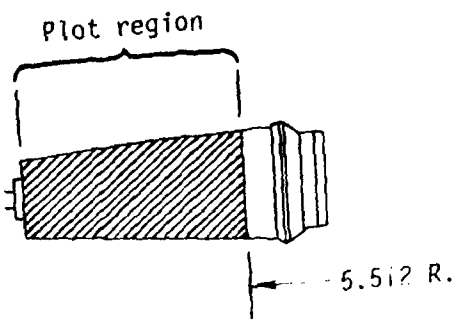
REV SYM

BOEING

NO D6-42735
PAGE 57



J16-047



Leading edge
Stress contours, ksi

Figure B.15 Equivalent Stress, Aero Load, Pressure Side, Set 3

01 4100 7740 ORIG. 8/21

REV SYM



J18-047

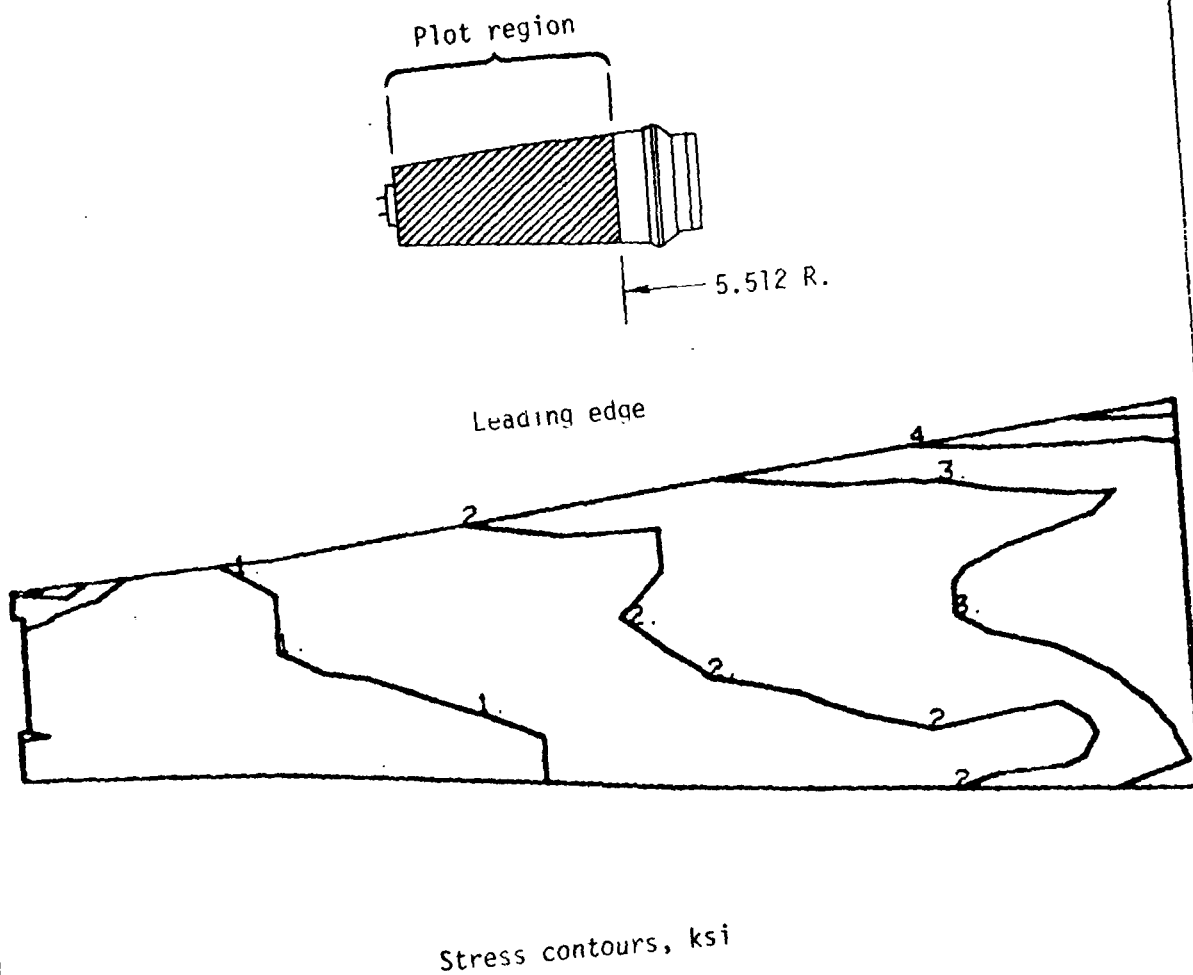


Figure B.16 Equivalent Stress, Aero Load, Suction Side, Set 3

D14100 7740 ONIG. B/71

REV SYM

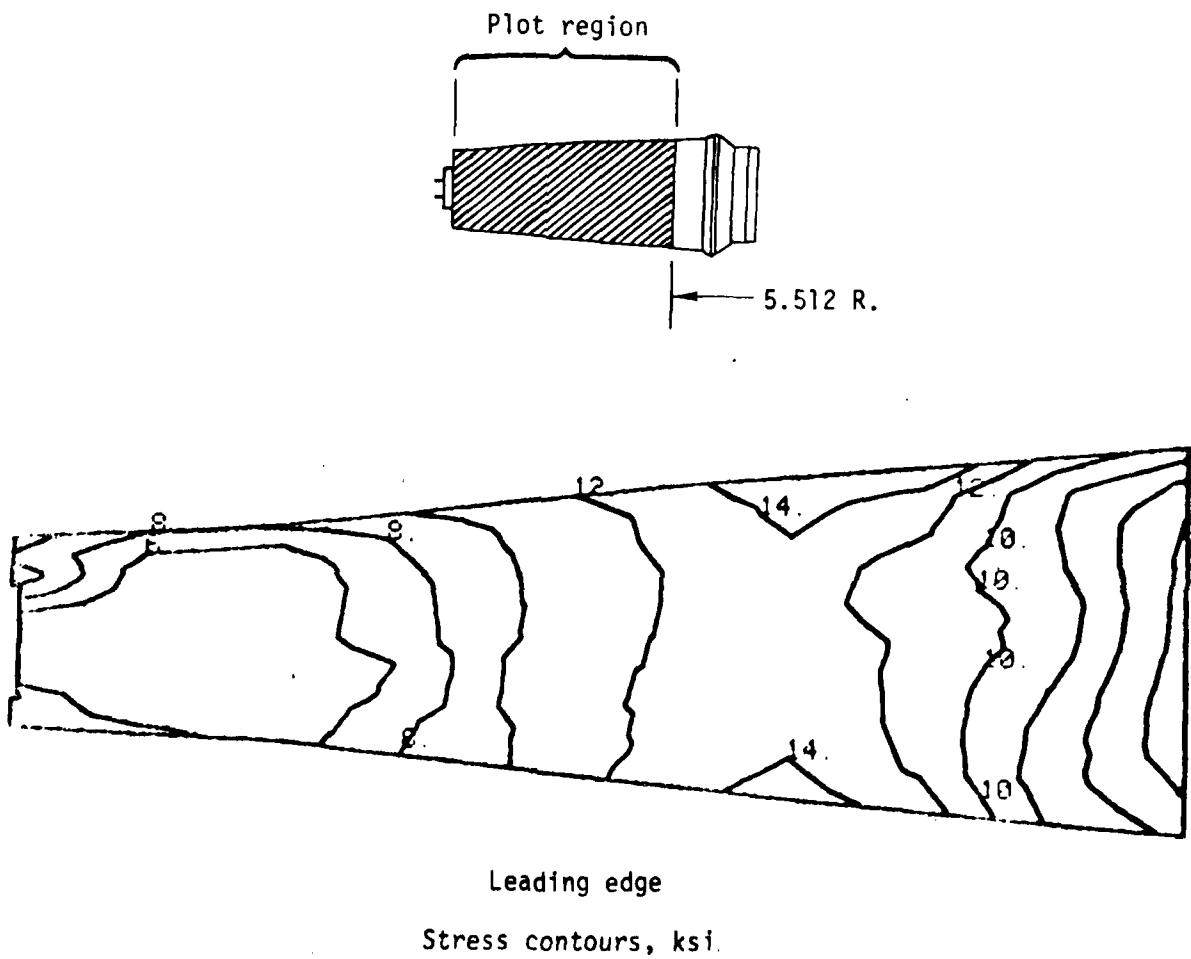
BOEING

NO. D6-42735

PAGE 59



J18-047



Leading edge
Stress contours, ksi.

Figure B.17 Equivalent Stress, Thermal Load, Pressure Side, Set 3

01 4 198 7748 ORIG. 8/71



J18-CA7

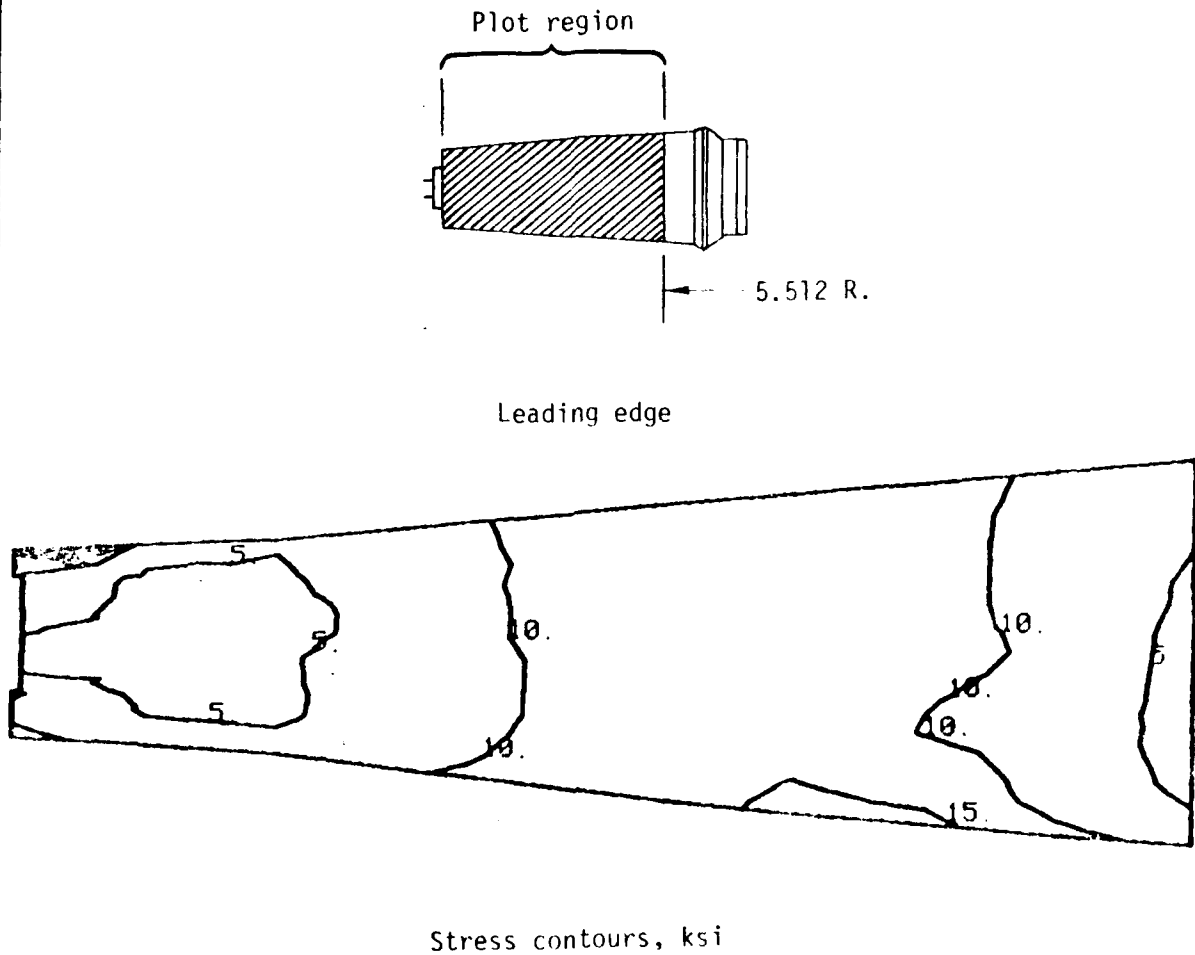


Figure B.18 Equivalent Stress, Thermal Load, Suction Side, Set 3

21 4 00 2740 OR.G.3/71



J18-047

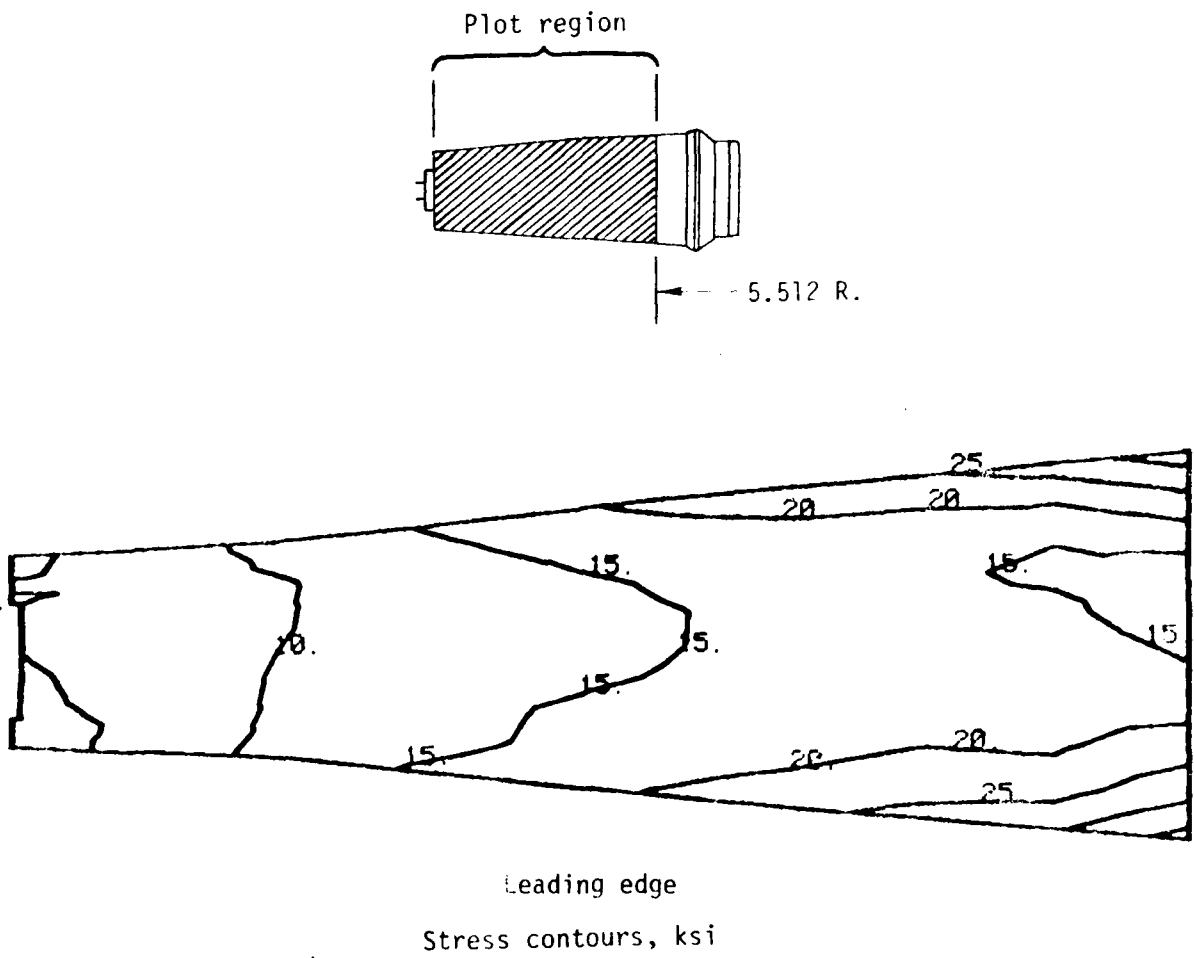


Figure B.19 Equivalent Stress, Tip Rub Load, Pressure Side, Set 3

014100 7740 OR G. 8/71



J18-047

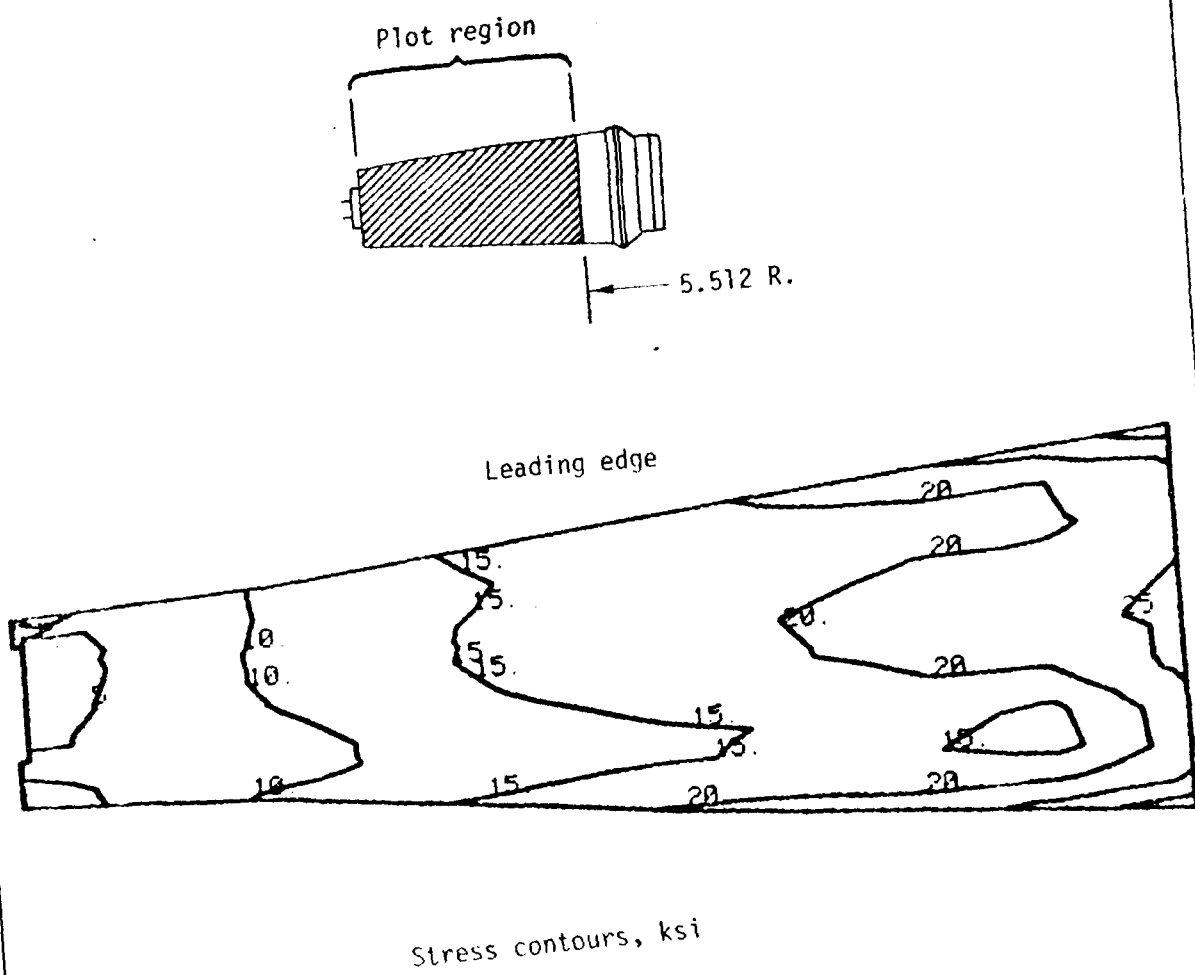


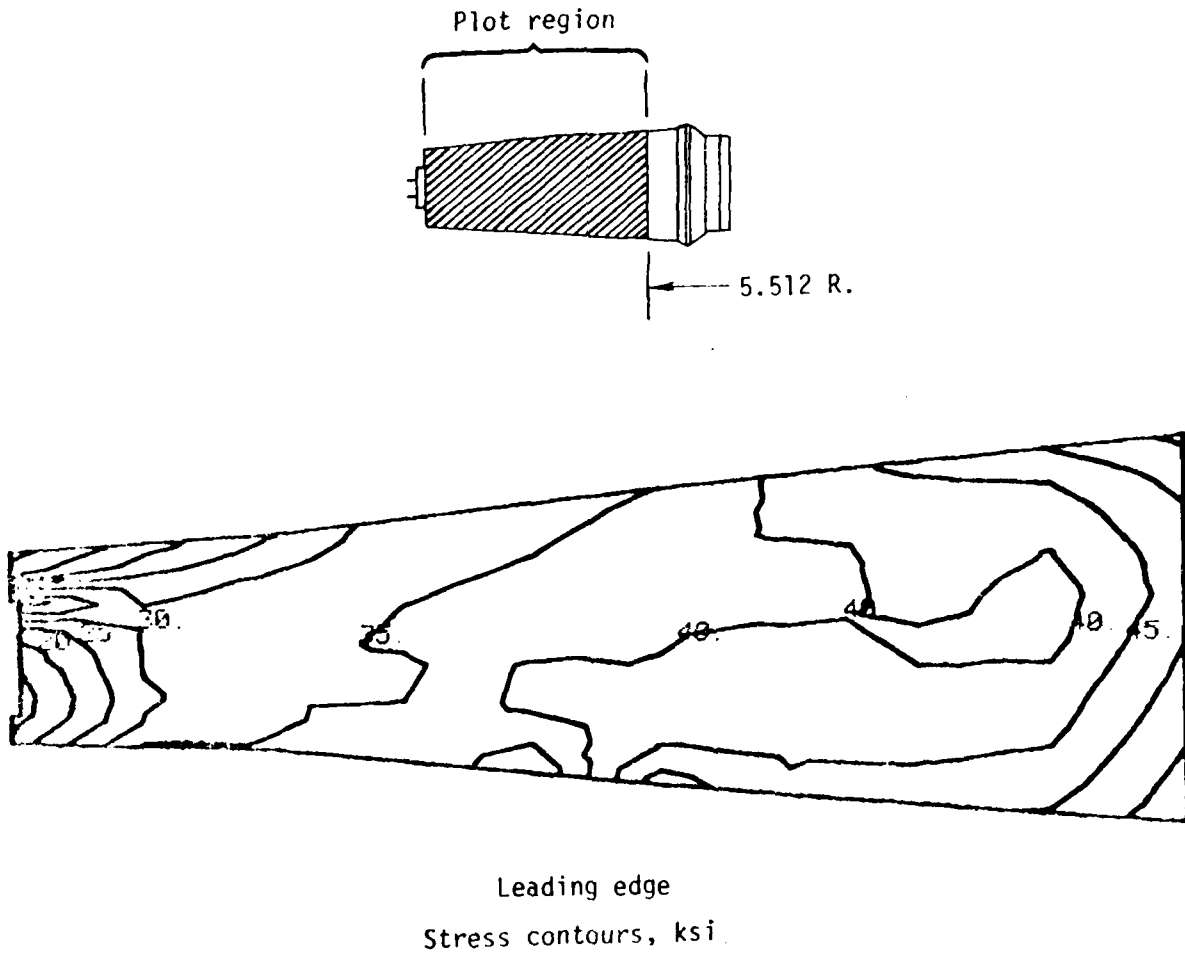
Figure B.20 Equivalent Stress, Tip Rub Load, Suction Side, Set 3

D1 8100 7740 ONI G. 3/71

REV SYM



J18-047



01 4 100 7740 ORIG. 2/71

Figure B.21 Equivalent Stress, CF + Aero + Thermal Loads, Pressure Side, Set 3

REV SYM

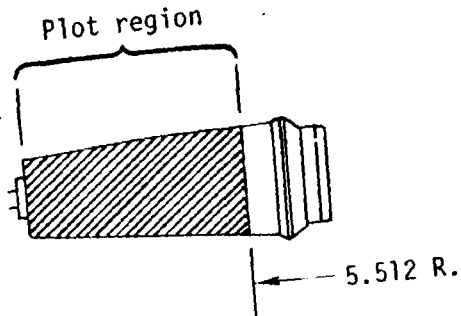
BOEING

NO. D6-42735

PAGE 64



J16-047



Leading edge

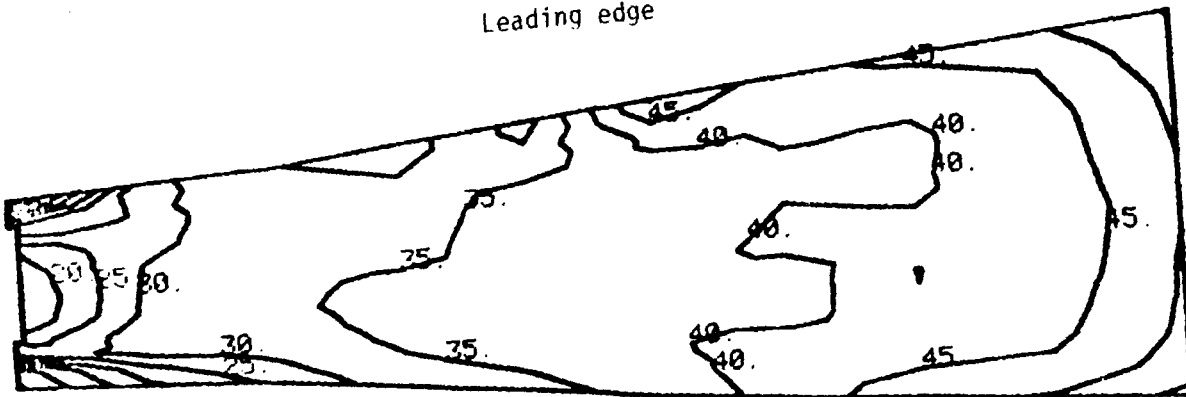


Figure B.22 Equivalent Stress, CF + Aero + Thermal Load, Suction Side, Set 3

DL 8100 7740 ORIG. 2/71

REV SYM

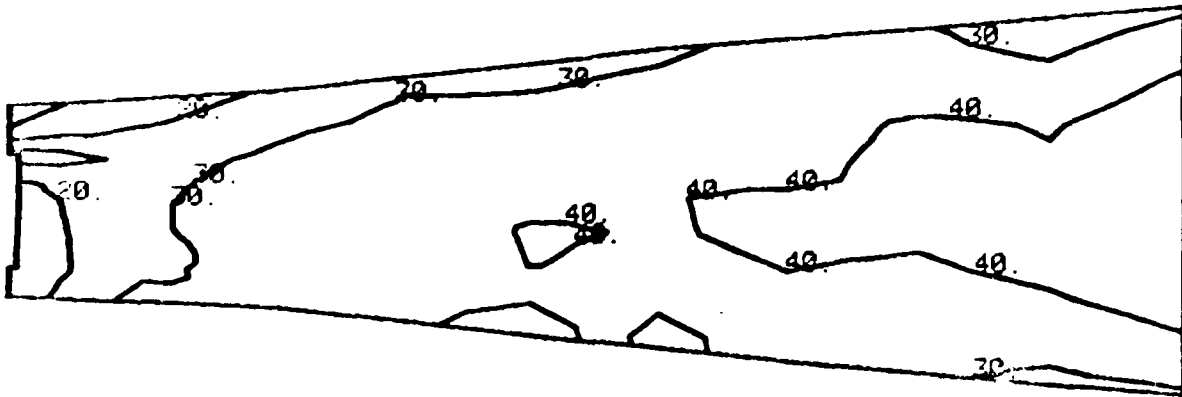
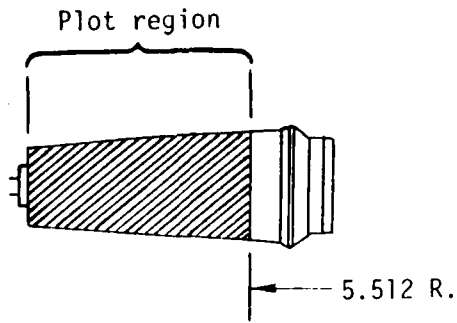
BOEING

NO. D6-42735

PAGE 65



J16-047

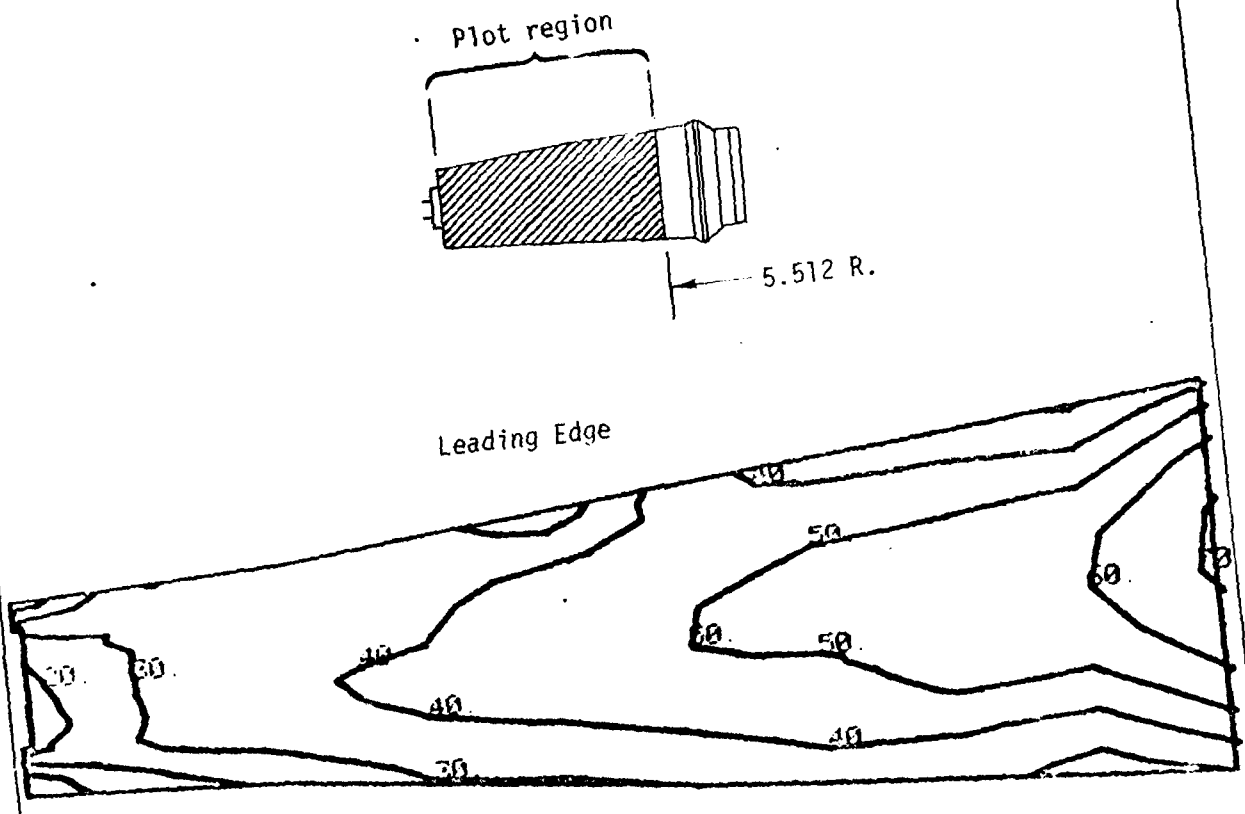


D1 4100 7740 ORIG. 3/71

Figure B.23 Equivalent Stress, CF + Aero + Thermal + Rub Load, Pressure Side, Set 3



J18-047



Stress contours, ksi

Figure B.24 Equivalent Stress, CF + Aero + Thermal + Rub Lead, Suction Side Set 3

D14 00 3740 ORIG. 2/71

REV SYM

BOEING

NO. D6-42735
PAGE 67



DISTRIBUTION LIST

No. of Copies	To
	Commander, US Army Aviation Systems Command, P.O. Box 209, St. Louis, Missouri 63166
10	ATTN: DRSAB-EXT
1	DRSAV-FE (Cliff Sims, Maint Engr)
1	DRSAV-EQ (C. Crawford, Sys Dev & Qual)
1	DRSAV-FES (H. Bull, Corpus Christi)
2	DRSAV-ZDR (Ref Library)
	Project Manager, Advanced Attack Helicopter, P.O. Box 209, St. Louis, Missouri 63166
1	ATTN: DRCPM-AAH, TM
	Project Manager, Utility Tactical Transport Aircraft System, P.O. Box 209, St. Louis, Missouri 63166
1	ATTN: DRCPM-UA-T
	Project Manager, CH-47 Modernization, P.O. Box 209, St. Louis, Missouri 63166
1	ATTN: DRCPM-CH47M
	Project Manager, Advanced Scout Helicopter, P.O. Box 209, St. Louis, Missouri 63166
1	ATTN: DRSAB-SIA
	Project Manager, Aircraft Survivability Equipment, P.O. Box 209, St. Louis, Missouri 63166
1	ATTN: DRCPM-ASE-TM
	Project Manager, Cobra, P.O. Box 209, St. Louis, Missouri 63166
1	ATTN: DRCPM-CO-T
	Project Manager, Iranian Aircraft Program, P.O. Box 209, St. Louis, Missouri 63166
1	ATTN: DRCPM-IAP-T
	Commander, US Army Materiel Development and Readiness Command, 5001 Eisenhower Avenue, Alexandria, Virginia 22333
4	ATTN: DRCLDC-TE
1	DRCLDC, Mr. R. Zentner
	Director, Eustis Directorate, US Army Air Mobility R&D Lab, Ft. Eustis, Virginia 23604
1	ATTN: SAVDL-EU-TAS
1	SAVDL-EU-SS, Mr. J. Robinson
	Director, Ames Directorate, US Army Air Mobility R&D Lab, Ames Research Center, Moffett Field, California 94035
1	ATTN: SAVDL-AM

No. of
Copies

To

Director, Langley Directorate, US Army Air Mobility R&D Lab,
Mail Stop 266, Hampton, Virginia 23365
1 ATTN: SAVDL-LA

Director, Lewis Directorate, US Army Air Mobility R&D Lab,
21000 Brook Park Rd, Cleveland, Ohio 44135
1 ATTN: SAVDL-LE

U. S. Army Industrial Base Engineering Activity, Rock Island, Illinois 61201
1 ATTN: DRXIB-MT, Mr. James W. Carstens, Chief, Manufacturing Tech. Division

Air Force Materials Laboratory, Manufacturing Technology Division
Wright-Patterson Air Force Base, Ohio 45433
1 ATTN: AFML/LTM
1 AFML/LTN
1 AFML/LTE

Commander, US Army Electronics Command, Ft. Monmouth, New Jersey 07703
1 ATTN: DRSEL-RD-P
1 DRSEL-GG-DD

Commander, US Army Missile Command, Redstone Arsenal, Alabama 35809
1 ATTN: DRSMI-IIE
1 Technical Library
1 DRSMI-RSM, Mr. E. J. Wheelahan

Commander, US Army Troop Support Command, 4300 Goodfellow Blvd.,
St. Louis, Missouri 63120
1 ATTN: DRSTS-PLC

Commander, US Army Armament Command, Rock Island, Illinois 61201
1 ATTN: DRSAR-PPR-1W
2 Technical Library

Commander, US Army Tank-Automotive Command, Warren, Michigan 48090
1 ATTN: DRDTA-RCM.1
2 DRDTA, Research Library

12 Commander, Defense Documentation Center, Cameron Station, Building 5,
5010 Duke Street, Alexandria, Virginia 22314

Hughes Helicopter, Division of Summa Corporation, M/S T-419, Centinella
Avenue and Teale Street, Culver City, California 90230
2 ATTN: Mr. R. E. Moore, Bldg. 314

Sikorsky Aircraft Division, United Aircraft Corporation,
Stratford, Connecticut 06497
2 ATTN: Mr. Stan Silverstein, Section Supv., Manufacturing Technology

No. of Copies	To
2	Bell Helicopter Company, P.O. Box 482, Ft. Worth, Texas 76101 ATTN: Mr. P. Baumgartner, Chief, Manufacturing Technology
2	Kaman Aerospace Corporation, Bloomfield, Connecticut 06002 ATTN: Mr. A. S. Falcone, Chief of Materials Engineering
2	Boeing Vertol Company, Box 16858, Philadelphia, Pennsylvania 19142 ATTN: R. Pinckney, Manufacturing Technology
2	Detroit Diesel Allison Division, General Motors Corporation, P.O. Box 894, Indianapolis, Indiana 46206 ATTN: James E. Knott, General Manager
2	General Electric Company, 10449 St. Charles Rock Road, St. Ann, Missouri 63074 ATTN: Mr. H. Franzen
2	AVCO-Lycoming Corporation, 550 South Main Street, Stratford, Connecticut 06497 ATTN: Mr. V. Strautman, Manager, Process Technology Laboratory
2	United Technologies Corporation, Pratt & Whitney Aircraft Division, Manufacturing Research and Development, East Hartford, Connecticut 06108 ATTN: Mr. Ray Traynor
2	Director, Army Materials and Mechanics Research Center, Watertown, Massachusetts 02172 ATTN: DRXMR-PL
1	DRXMR-AG
1	DRXMR-PR
1	DRXMR-CT
1	DRXMR-X
1	DRXMR-AP
1	DRXMR-M
1	Author

UNCLASSIFIED
UNLIMITED DISTRIBUTION
Key Words
Stress analysis
Finite element method
Gas turbine blades

Amy Materials and Mechanics Research Center,
Watertown, Massachusetts 02172
3-D STRESS ANALYSIS OF A TURBINE BLADE -
C. M. Lewis, R. A. Samuel, and F. Yen
Boeing Commercial Airplane Company,
Seattle, Washington 98124

Technical Report AMMRC CTR 77-14, March 1977, 77 pp -
illus - tables, AMCMS Code 738017.A50Q3019-WF-3MS
Final Report

This report presents a demonstration of the usefulness of the ATLAS system in performing three-dimensional elastic stress analysis of a turbine blade. Modeling details for a shrouded uncooled turbine blade are outlined and program execution and data management techniques are discussed. It was concluded that three-dimensional elastic stress analysis provides an accurate means of predicting stresses in a complex structure. However, high computer costs require that this method of stress analysis be used with discretion. Areas for further study are suggested.

UNCLASSIFIED
UNLIMITED DISTRIBUTION
Key Words
Stress analysis
Finite element method
Gas turbine blades

Amy Materials and Mechanics Research Center,
Watertown, Massachusetts 02172
3-D STRESS ANALYSIS OF A TURBINE BLADE -
C. M. Lewis, R. A. Samuel, and F. Yen
Boeing Commercial Airplane Company,
Seattle, Washington 98124

Technical Report AMMRC CTR 77-14, March 1977, 77 pp -
illus - tables, AMCMS Code 738017.A50Q3019-MS-3MS
Final Report

This report presents a demonstration of the usefulness of the ATLAS system in performing three-dimensional elastic stress analysis of a turbine blade. Modeling details for a shrouded uncooled turbine blade are outlined and program execution and data management techniques are discussed. It was concluded that three-dimensional elastic stress analysis provides an accurate means of predicting stresses in a complex structure. However, high computer costs require that this method of stress analysis be used with discretion. Areas for further study are suggested.

UNCLASSIFIED
UNLIMITED DISTRIBUTION
Key Words
Stress analysis
Finite element method
Gas turbine blades

Amy Materials and Mechanics Research Center,
Watertown, Massachusetts 02172
3-D STRESS ANALYSIS OF A TURBINE BLADE -
C. M. Lewis, R. A. Samuel, and F. Yen
Boeing Commercial Airplane Company,
Seattle, Washington 98124

Technical Report AMMRC CTR 77-14, March 1977, 77 pp -
illus - tables, AMCMS Code 738017.A50Q3019-MS-3MS
Final Report

This report presents a demonstration of the usefulness of the ATLAS system in performing three-dimensional elastic stress analysis of a turbine blade. Modeling details for a shrouded uncooled turbine blade are outlined and program execution and data management techniques are discussed. It was concluded that three-dimensional elastic stress analysis provides an accurate means of predicting stresses in a complex structure. However, high computer costs require that this method of stress analysis be used with discretion. Areas for further study are suggested.

UNCLASSIFIED
UNLIMITED DISTRIBUTION
Key Words
Stress analysis
Finite element method
Gas turbine blades

Amy Materials and Mechanics Research Center,
Watertown, Massachusetts 02172
3-D STRESS ANALYSIS OF A TURBINE BLADE -
C. M. Lewis, R. A. Samuel, and F. Yen
Boeing Commercial Airplane Company,
Seattle, Washington 98124

Technical Report AMMRC CTR 77-14, March 1977, 77 pp -
illus - tables, AMCMS Code 738017.A50Q3019-MS-3MS
Final Report

This report presents a demonstration of the usefulness of the ATLAS system in performing three-dimensional elastic stress analysis of a turbine blade. Modeling details for a shrouded uncooled turbine blade are outlined and program execution and data management techniques are discussed. It was concluded that three-dimensional elastic stress analysis provides an accurate means of predicting stresses in a complex structure. However, high computer costs require that this method of stress analysis be used with discretion. Areas for further study are suggested.

Army Materials and Mechanics Research Center,
Watertown, Massachusetts 02172
3-D STRESS ANALYSIS OF A TURBINE BLADE -
C. M. Lewis, R. A. Samuel, and F. Yen
Boeing Commercial Airplane Company,
Seattle, Washington 98124

Technical Report AMMRC CTR 77-14, March 1977, 77 pp -
illus - tables, AMCMS Code 738017.A50Q3019-MS-3MS
Final Report

This report presents a demonstration of the usefulness of the ATLAS system in performing three-dimensional elastic stress analysis of a turbine blade. Modeling details for a shrouded uncooled turbine blade are outlined and program execution and data management techniques are discussed. It was concluded that three-dimensional elastic stress analysis provides an accurate means of predicting stresses in a complex structure. However, high computer costs require that this method of stress analysis be used with discretion. Areas for further study are suggested.

UNCLASSIFIED
UNLIMITED DISTRIBUTION
Key Words
Stress analysis
Finite element method
Gas turbine blades

Army Materials and Mechanics Research Center,
Watertown, Massachusetts 02172
3-D STRESS ANALYSIS OF A TURBINE BLADE -
C. M. Lewis, R. A. Samuel, and F. Yen
Boeing Commercial Airplane Company,
Seattle, Washington 98124

Technical Report AMMRC CTR 77-14, March 1977, 77 pp -
illus - tables, AMCMS Code 738017.A50Q3019-MS-3MS
Final Report

This report presents a demonstration of the usefulness of the ATLAS system in performing three-dimensional elastic stress analysis of a turbine blade. Modeling details for a shrouded uncooled turbine blade are outlined and program execution and data management techniques are discussed. It was concluded that three-dimensional elastic stress analysis provides an accurate means of predicting stresses in a complex structure. However, high computer costs require that this method of stress analysis be used with discretion. Areas for further study are suggested.

UNCLASSIFIED
UNLIMITED DISTRIBUTION
Key Words
Stress analysis
Finite element method
Gas turbine blades

Army Materials and Mechanics Research Center,
Watertown, Massachusetts 02172
3-D STRESS ANALYSIS OF A TURBINE BLADE -
C. M. Lewis, R. A. Samuel, and F. Yen
Boeing Commercial Airplane Company,
Seattle, Washington 98124

Technical Report AMMRC CTR 77-14, March 1977, 77 pp -
illus - tables, AMCMS Code 738017.A50Q3019-MS-3MS
Final Report

This report presents a demonstration of the usefulness of the ATLAS system in performing three-dimensional elastic stress analysis of a turbine blade. Modeling details for a shrouded uncooled turbine blade are outlined and program execution and data management techniques are discussed. It was concluded that three-dimensional elastic stress analysis provides an accurate means of predicting stresses in a complex structure. However, high computer costs require that this method of stress analysis be used with discretion. Areas for further study are suggested.

UNCLASSIFIED
UNLIMITED DISTRIBUTION
Key Words
Stress analysis
Finite element method
Gas turbine blades

Army Materials and Mechanics Research Center,
Watertown, Massachusetts 02172
3-D STRESS ANALYSIS OF A TURBINE BLADE -
C. M. Lewis, R. A. Samuel, and F. Yen
Boeing Commercial Airplane Company,
Seattle, Washington 98124

Technical Report AMMRC CTR 77-14, March 1977, 77 pp -
illus - tables, AMCMS Code 738017.A50Q3019-MS-3MS
Final Report

This report presents a demonstration of the usefulness of the ATLAS system in performing three-dimensional elastic stress analysis of a turbine blade. Modeling details for a shrouded uncooled turbine blade are outlined and program execution and data management techniques are discussed. It was concluded that three-dimensional elastic stress analysis provides an accurate means of predicting stresses in a complex structure. However, high computer costs require that this method of stress analysis be used with discretion. Areas for further study are suggested.

UNCLASSIFIED
UNLIMITED DISTRIBUTION
Key Words
Stress analysis
Finite element method
Gas turbine blades

ANMRC CTR 77-14

THIRD STRESS ANALYSIS OF A TURBINE BLADE

Lewis, Samuel and Yen

DEPARTMENT OF THE ARMY
ARMY MATERIALS AND MECHANICS RESEARCH CENTER
Watertown, Massachusetts 02172
OFFICIAL BUSINESS

POSTAGE AND FEES PAID
DEPARTMENT OF THE ARMY
DOD 314

THIRD CLASS MAIL